On the Stereoselective Pharmacokinetics of Eflornithine and Prediction of Drug Tissue to Plasma Concentration Ratios

Rasmus Jansson Löfmark

2009

UNIVERSITY OF GOTHENBURG

Department of Pharmacology
Institute of Neuroscience and Physiology
The Sahlgrenska Academy at University of Gothenburg
Sweden

Till Cajsa

On the Stereoselective Pharmacokinetics of Eflornithine and Prediction of Drug Tissue to Plasma Concentration Ratios

Abstract

Eflornithine is one of two registered drugs for the treatment of late-stage human African trypanosomiasis, a uniformly fatal neglected disease with sixty million people are at risk of being infected. Eflornithine is efficacious but the cumbersome intravenous administration leaves numerous patients untreated. A simplified mode of administration, preferably oral, would enable more patients having access to treatment. The trypanostatic agent eflornithine is administered as a racemate where the L – form has a several-fold greater *in vitro* potency compared to the D – enantiomer. Despite the difference in potency of the enantiomers, the stereoselective pharmacokinetics of eflornithine has not been considered.

This thesis aimed to study L – and D – eflornithine pharmacokinetics in the rat, in Caco-2 cells and in late-stage human African Trypanosomiasis patients. A secondary aim was also to develop a general method for predicting drug tissue to plasma concentration ratios.

In the rat, eflornithine displayed stereoselective absorption where the more potent L – form had an approximately 50% lower fraction absorbed compared to D – eflornithine. The stereoselective mechanism was not detected in the present Caco-2 cell assay. Late-stage HAT patients, treated with racemic oral eflornithine, had an approximate 50% lower exposure of L – compared to D – eflornithine, similar to those in rat. The findings suggested that previous attempts to develop an oral eflornithine dosage regimen have failed due to unfavorable stereoselective absorption. High plasma exposure for both L – and D – eflornithine were significantly correlated to the probability of being cured.

For the secondary aim of this thesis, the novel method to predict drug tissue distribution, based on a measured volume of distribution in combination with drug lipophilicity performed reasonably well. Predicted drug tissue to plasma concentration ratios agreed reasonably well with experimentally determined values with 85% being within a factor of ±3 to experimental values (n=148).

In conclusion, this thesis present the stereoselective pharmacokinetics of eflornithine that can give information on whether a much needed oral eflornithine can be developed or not. In addition, the thesis also presents a general method to predict drug tissue to plasma concentration ratios.

Keywords: Human African trypanosomiasis, HAT, pharmacokinetics, NONMEM, stereoselectivity, eflornithine, tissue distribution

Eflornitins stereoselektiva farmakokinetik och förutseendet av substansers vävnadsfördelning

Swedish summary - Populärvetenskaplig sammanfattning

Farmakokinetik är det vetenskapsområde som redogör för hur läkemedel tas upp, fördelas, bryts ner och utsöndras ur kroppen. Fördelningsvolymen är ett mått som visar hur mycket läkemedel som fördelas ut i kroppen. Man beräknar fördelningsvolymen genom att mäta plasmakoncentrationen efter en intravenös dos av läkemedel. Fördelningen av ett läkemedel till en specifik vävnad kallas för Kp-värde och mäts vanligtvis genom att ta kvoten av vävnads- och plasmakoncentrationen. En kiral substans är en substans som förenklat kan beskrivas som två former där den ena är högervriden och den andra vänstervriden.

Denna avhandling hade i huvudsak två syften. Den ena var att utveckla en metod för att, utifrån fördelningsvolymen kombinerat med läkemedlets fettlöslighet, kunna förutse läkemedlets specifika Kp-värden. Den framtagna metoden skiljer sig från tidigare tillvägagångssätt inom området och kan vara användbar i utvecklingen av nya läkemedel.

Det andra syftet var att undersöka den kirala farmakokinetiken för eflornitin i råtta, cellkulturer och slutligen i människa för att utvärdera möjligheten att ta fram en förenklad behandling mot afrikansk sömnsjuka. Eflornitin är ett av två registrerade läkemedel som används vid behandling mot det sena stadiet av human afrikansk sömnsjuka. Parasitsjukdomen anses vara försummad, är i stort sett alltid dödlig vid utebliven behandling och påverkar cirka 60 miljoners människors liv. Eflornitin är effektivt men administreringen är omständig, vilket har lett till att många patienter inte får behandling. En förenklad behandling skulle således kunna möjligöra att fler patienter får tillgång till behandling och bli botade. Eflornitin administreras som ett racemat, en 50:50 blandning av en höger- och vänstervriden form. Cellstudier har visat att den såkallade L-formen är flerfaldigt mer aktiv jämfört med den andra formen. De olika formernas potens har tidigare inte beaktats vid försök att förenkla behandlingen.

Metoden som utvecklades för att förutse substansers vävnadsfördelning, fungerade relativt bra och kunde förutsäga 85 procent av experimentella värden, inom en faktor ± tre. Upptaget av eflornitin i råttans mage-tarm visade sig vara en kiral process där den mer potenta L-formen enbart togs upp till hälften jämfört med den mindre potenta formen. Denna kirala process kunde dock inte visas i cellkulturer. Hos patienter med afrikansk sömnsjuka, som behandlades med eflornitin oralt, var plasmaexponering för L-formen hälften av den mindre potenta D-formen. Detta var troligtvis orsakat av ett kiralt upptag över mage-tarm kanalen. Plasmaexponering av både den aktiva formen och summan av de båda formerna visade sig vara signifikant korrelerade till sannolikheten att bli botad.

Sammanfattningsvis presenterar denna avhandling forskningsresultat inom två områden. Inledningsvis redogörs för en metod som används för att förutsäga läkemedels fördelning ut till olika vävnader. I den andra delen presenteras den kirala farmakokinetiken för eflornitin, som delvis kan ligga till grund för en eventuell utveckling av en oral behandling mot afrikansk sömnsjuka.

Papers Discussed

This thesis is based on the following papers, which will be referred to in the text by the roman numerals assigned to them below.

I.   **Jansson R**., Bredberg U., Ashton M. Prediction of drug tissue to plasma concentration ratios using a measured volume of distribution in combination with lipophilicity. *Journal of Pharmaceutical Sciences*, 2008 Jun;97(6):2324-39

II.   **Jansson R**., Malm M., Roth C., Ashton M. Enantioselective and nonlinear intestinal absorption of eflornithine in the rat. *Antimicrobial Agents and Chemotherapy,* 2008 Aug;52 (8):2842-8.

III.   **Jansson-Löfmark R**., Römsing S., Albers E., Ashton M. Determination of eflornithine enantiomers in plasma, by precolumn derivatization with o-phtaladehyde-N-acetyl-L-cysteine and liquid chromatography with UV-detection. *Submitted*

IV.   **Jansson-Löfmark R**., Johansson C-C., Hubatsch I., Artursson P., Ashton M. Investigations of the enantioselective absorption and pharmacokinetics of eflornithine in the rat and bidirectional permeabilities in Caco-2 cells. *In manuscript*

V.   **Jansson-Löfmark R**., Björkman S., Na-Bangchang K., Doua F., Ashton M. Enantiospecific reassessment of the pharmacokinetics and pharmacodynamics of oral eflornithine against late-stage *T.b. gambiense* sleeping sickness. *In manuscript*

Table of Contents

List of Abbreviations

AUC   = area under the drug concentration-time curve
DFMO   = eflornithine
CL   = clearance
CSF   = cerebrospinal fluid
F   = bioavailability
HPLC   = high performance liquid chromatography
IIV   = interindividual variability
Ka   = first-order absorption rate constant
Kp   = drug tissue to plasma concentration ratio at equilibrium
LOD   = limit of detection
logD7.4   = logarithmic value of octanol:water partitioning at pH 7.4
logP   = logarithmic value of octanol:water partitioning
LOQ   = limit of quantitation
MTT   = mean transit time
OFV   = objective function value
P-gp   = P-glycoprotein
PK   = pharmacokinetics
Q   = intercompartmental clearance
QC   = quality control
RSD   = relative standard deviation
RSE   = relative standard error
SD   = standard deviation
SSR   = sum of square residuals
UV   = ultraviolet
Vc   = central volume of distribution
Vp   = peripheral volume of distribution
VPC   = visual predictive check
Vss   = volume of distribution at steady state
WHO   = World Health Organization

Introduction

Background

Pharmacokinetics is the study of the fate of pharmaceutical compounds in the body and often uses a mathematical description to analyze, interpret and model the time-course of drugs. It is usually studied in conjunction with pharmacodynamics which deals with the study of the time course of drug effects, and the relationship between effect and exposure[1]. Pharmacokinetics can therefore be considered as the science that links the administered drug to its pharmacodynamics. This link makes pharmacokinetics a critical part in aspects such as drug development, dose optimization and individual dose adjustments. Pharmacokinetics can be subdivided in terms of absorption, distribution, metabolism and excretion of compounds.

The extent of drug tissue distribution is characterized by an equilibrium partitioning constant (Kp) describing the ratio between tissue and plasma drug concentrations. Measuring tissue concentrations can be time-consuming and reliable methods to predict tissue distribution would be highly beneficial. Tissue-specific Kp values are also one of the main parameters needed in whole body physiologically based pharmacokinetic (PBPK) models.

Eflornithine is one of two drugs registered for the treatment of late-stage human African trypanosomiasis, a uniformly fatal disease if left untreated [2]. Eflornithine is more frequently recommended as a first line treatment but due to its complicated intravenous administration, numerous patients are left untreated [3,4]. A simplified mode of administration would enable more patients having access to treatment. Eflornithine is available as a racemate, a 50:50 mixture of the complementary enantiomers, and it has been shown that, compared to D-eflornithine, the L – enantiomer is more potent for the target enzyme ornithine decarboxylase and a similar stereoselectivity have been observed in cultured *Trypanosomas brucei* parasites [5] (R.Brun, Swiss Tropical Institute, personal communication). Considering this, the stereoselective pharmacokinetics was investigated to find possible solutions for the development of a more simplified mode of administration.

The thesis starts from a wide perspective focusing on aspects of tissue distribution and eventually narrows down to the stereoselective pharmacokinetics of eflornithine and its possible consequences for the development of an oral treatment of late-stage human African trypansomiasis infected patients.

Tissue distribution

Tissue-to-plasma drug concentration ratios are important parameters that in part govern the fate of drugs in the body. They are also required in whole body physiologically based pharmacokinetic models [6, 7]. Physiologically based pharmacokinetic models strive to mechanistically describe the anatomical, physiological, physical, and chemical descriptions of the fate of the drug in the body. One of the applications of PBPK models is the possibility to scale up and predict human pharmacokinetics for new compounds under development. However, one of the limiting factors with PBPK models is the number of drug-specific input parameters required. One of these parameters are drug tissue-to-plasma concentration ratios. Experimental determination of these parameter is a time-consuming and laborious task. Having accurate methods to predict tissue-to-plasma drug concentration ratios would be highly beneficial.
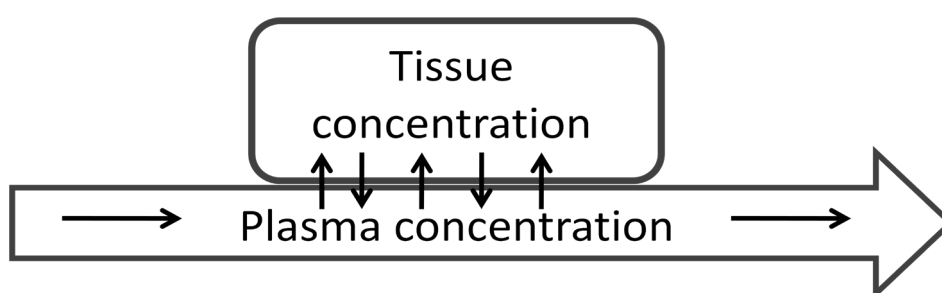

Figure 1. Tissue-to-plasma drug concentration ratio (Kp value). The Kp value can be calculated by dividing the tissue concentration by the plasma concentration, when conditions are under steady state.

There are mechanistic based models, requiring *in vitro* data (plasma protein binding, blood-plasma ratio), for prediction of Kp values available. The method that was developed by Poulin and Theil was based upon tissue composition (lipid, water, and phospholipid content), compound lipophilicity and plasma protein binding [8-11]. This approach has been further modified by Berezhkovskiy [12]. In addition to these methods, Rodgers and Rowland have further developed methods to predict Kp values. For moderate to strong bases electrostatic interaction was taken into account by using the tissue acidic phospholipid content and this interaction was derived from blood cell partitioning. For acids, zwitterions, weak bases and neutrals the albumin or lipoprotein content was taken into account and the interaction was derived from plasma protein binding [13-15].

These methods are generated upon *in vitro* (i.e. plasma protein binding, blood cell binding and compound lipophilicity) data for prediction of tissue distribution and hence volume of distribution. However, once an *in vivo* estimate of the volume of distribution, in an experimental animal species, has been obtained this information could be used if it leads to an improved prediction of tissue partitioning.

Volume of distribution at steady state (Vss), correspond to the sum of the plasma volume and the apparent volumes for all tissues. The apparent volume for a tissue, for a particular

12

compound, is the determined by its Kp value and its physiological volume[12]. There are methods to predict tissue-to-plasma concentration ratios, using Vss, for the implementation in PBPK models [16],[17]. However both of these proposed methods were based on merely 10 – 15 structurally unrelated compounds.

Stereoselectivity in pharmacokinetics

Many of the currently available drugs are chiral, and are administered as a racemate, meaning a 50:50 mixture of their complementary enantiomers. In biological systems, the three-dimensional structure of proteins make them highly stereospecific and their interaction with enantiomeric compound can differ leading to stereoselective pharmacokinetics and pharmacodynamics[18-21]. Regarding distribution, there are a several cases where stereoselective binding to proteins can turn into stereoselective pharmacokinetic behavior, such as in the case of methadone[22]. Chloroquine has been shown to have a stereoselective plasma protein binding [23, 24] and there are also cases where disease states and age can influence the stereoselectivity in pharmacokinetics [25]. For metabolism it is quite common to see differences *in vitro* with regards to enzyme affinity (*i.e.* Km) and the maximum metabolic rate (*i.e.* Vmax) explaining different *in vivo* clearance of the enantiomers. Absorption processes usually involve a passive transfer across membranes making stereoselective absorption less common. Stereoselective drug absorption usually implies that some form of active transport is involved. P-glycoprotein (P-gp) has been shown to display stereoselectvie efflux [26]. There are also examples of active carrier-mediated stereoselective absorption in Caco-2 cells [27].

Gastrointestinal absorption

Oral administration is the most common drug delivery route. It usually preferred by patients and also enhances compliance. However, orally administered drugs will need to pass a number of barriers before the drug can reach the systemic circulation. The fraction of an oral dose that reaches systemic circulation in its unmetabolised form is referred to as bioavailability (F). Bioavailability is a function of the fraction of the drug that is absorbed across the apical membrane of the enterocytes (Fabs), the fraction of the dose that is not metabolised in the gut wall (Fgut) and the fraction that escapes metabolism and biliary excretion in the liver (Fh) [28].

Intestinal Lumen (apical side)

1. Passive transcellular
2. Transcytosis
3. Active carrier-mediated
4. Efflux
5. Metabolism
6. Passive paracellular
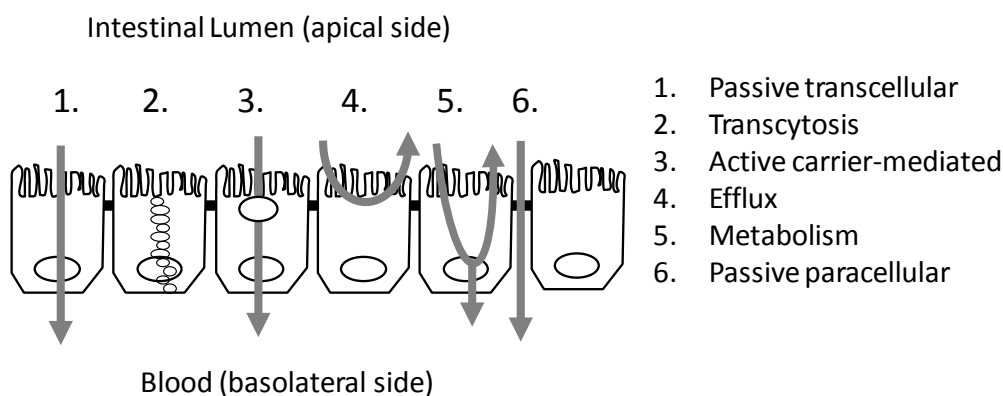
Blood (basolateral side)

Figure 2. Schematic illustration of the different intestinal drug transport mechanisms by the transcellular route (1-5) and paracellular route (6). Illustration adapted from Stenberg *et al* [29].

The absorption of small compounds across the intestinal epithelium has in general two different pathways; either through the epithelial cells (transcellular route) or between cells via tight junctions (paracellular route) (Figure 2). The transcellular route can either be driven by passive diffusion or by active carrier-mediated transport. Passive transcellular absorption is usually restricted to lipophilic molecules and is the most common way of absorption for orally administered drugs [29, 30]. Active carrier-mediated transport can be specific and highly selective for a number of chemical structures and sometimes operate in parallel with passive absorption mechanisms, such as in the case for ornithine[31]. It has been proposed that for large hydrophilic compounds (MW greater than 250 – 300) active-mediated transport is of importance [30, 32-36].

Transcytosis of exogenous compounds is a variation of the passive transcellular pathway and has been suggested to be limited and of relevance only for some macromolecules[37]. Efflux mechanisms across the gastrointestinal tract are driven by transporters located either on the apical or the basolateral side. A number of efflux transporters have been indentified and the most studied efflux transporter is P-glycoprotein. The presence and the expression of transporters have been shown to display regional differences [38, 39]. Gut epithelial metabolism has also been shown and is more commonly being observed and can affect the fraction absorbed. The most abundant isoforms among human P450 enzymes is CYP3A4 which has been reported to be about 70% of the total P450 content in the intestine [40].

Paracellular absorption is transport of drug through the intercellular spaces. The paracellular pathway occurs through tight junctions which constitute the major route-limiting barrier for the paracellular transport of ions and larger solutes [41]. The paracellular network is a rather complex system consisting of numerous proteins that form the junctional complex [42]. This pathway has been considered as a minor intestinal route of drug absorption for compounds with a molecular weight (MW) greater than 250 – 300 g/mol [34, 43]. However, the quantitative importance of paracellular route for the intestinal absorption of hydrophilic compounds *in vivo* is not yet fully clarified. *In vitro* studies have demonstrated that the paracellular route can be important for the intestinal absorption of various hydrophilic compounds. In addition, the paracellular route can also display nonlinear absorption kinetics [44].

14

Oral drug absorption is determined by the interaction of physicochemical properties of the compound and physiological characteristics of the gastrointestinal tract. The physicochemical properties of the compound, such as the molecular size, hydrogen bonding, conformation or lipophilicity (LogP, LogD) will direct whether a compound will be transported by the paracellular route or the transcellular route [36]. In addition, susceptibility of a drug to chemical degradation and stability can determine whether a compound is intact long enough for absorption to occur [45].

Human African trypanosomiasis

Human African trypanosomiasis (HAT), also known as sleeping sickness, is prevalent in 36 Sub-Saharan African countries. It has been reported that approximately sixty million people are at risk of being infected and it is considered as a neglected disease [46]. Neglected diseases are those that affect people in world's poorest populations for which satisfactory treatment does not exist and the required investments to generate new drugs is a major restriction [47]. HAT has also been ranked the third world's most important parasitic disease affecting human health after malaria and schistosomiasis, when adjusted for the number of years lost [2, 48].

During the first half of the twentieth century, HAT destroyed entire communities in central Africa. Then the disease was almost brought under control during the 1960s primarily thanks to highly effective surveillance programs[49]. Thereafter there was a gradual increase in the number of new cases and deaths. During the period 1986 to 2004, the world health organization estimated that there was an annual prevalence of 300,000 - 500,000 cases [46, 50, 51]. The primary cause was due to inadequate disease surveillance and treatment, particularly in Uganda, Angola, Sudan and Congo where the disease occurred in epidemics [52]. The disease incidence was estimated by the WHO in 2006 to 70,000 existing cases, however it is still difficult to provide accurate estimates of disease incidence and prevalence and there are also other reports suggesting lower numbers [51].

There are two forms of HAT; the West African form and the East African form. The East African contributes with less than 10% of the reported cases and is caused by the subspecie *Trypanosomas brucei rhodesiense (T.b.rhodesiense)*. The East African form causes an acute infection were the first symptoms are observed after a few weeks or months with parasites rapidly invading the central nervous system. The West African form, caused by the subspecies *T.b.gambiense*, give raise to a chronic infection where the patient can be infected for months or even years without major symptoms of the disease. When symptoms do emerge, the patient is often already in the late stage when the central nervous system has been invaded [53].

The disease, independent of form, is usually divided into two stages; an early hemolymphatic stage (first-stage) and a late encephalitic stage (late-stage) when the central nervous system has been invaded. The early symptoms are of a more non-specific type, such as malaise, headache, general weakness and weight loss. A number of organs may be infected such as the spleen, liver, skin, cardiovascular system, and the endocrine

system[48, 53]. In the late stage, when the parasites have invaded the central nervous system a wide array of neurological symptoms occur that can be categorized into psychiatric, motor, sensory abnormalities and sleep disturbances. The various features, including the sleep abnormalities, can be hard to diagnose, since some of these symptoms are also seen during other CNS infections. If untreated, the patient progresses to the final stage of the disease, which is characterized by seizures, severe somnolescence, incontinense, cerebral edema, coma, systemic organ failure and finally leads to death. The disease is said to have a 100% mortality, although the number has been debated [54].

Drug therapy for human African trypanosomiasis

There are currently four drugs available for the treatment of HAT. Suramin and pentamidine, used for the early stage, were introduced more than half a century ago. Melarsoprol and eflornithine are the two currently registered drugs for the late-stage. Melarsoprol has been in use since 1949, while eflornithine was registered in 1990 [55].

Melarsoprol is an arsenical drug that is useful for the treatment of late stage, for both of the *Trypanomas brucei* subspecie infections. The major problem with melarsoprol therapy is its toxicity and the risk of resistance[56-58]. There are a number of side effects of melarsoprol treatment with the worst adverse event being reactive encephalopathy, which occurs in 5 – 10 % of the patients treated, and results in death for 10 – 50% in those whom it develops.

Eflornithine

Eflornithine (D,L-α-difluoromethylornithine, DFMO) was initially developed as a potential anticancer drug in the early 1970s although never marketed for that use[59]. However, recent studies have shown that eflornithine, combined with sulindac, may be effective for the treatment of colon cancer and has shown promising results in clinical trials[60-64]. In addition to being a potential drug for treatment of colon cancer, eflornithine is also being sold as a facial hair cream remover under the trade name Vaniqa[65].

During the early 1980s it was found that eflornithine may be effective for the treatment of human African trypansomiasis [66]. In 1990, eflornithine was granted marketing approval and orphan drug status by the FDA, under the trade name Ornidyl.

Eflornithine is more frequently being recommended as first line treatment [56, 67, 68]. The most commonly used dosage regimen for the treatment of late stage HAT patients consists of 100 mg/kg body weight every 6th hour for 10 – 14 days given as short intravenous infusions[4]. For children a higher dose level is required, to achieve sufficient plasma and CSF concentrations, corresponding to 150 mg/kg body weight [69]. It is

currently administered alone although its combination with nifurtimox appears to be a promising approach for the treatment of late-stage HAT patients [70, 71].

The trypanostatic effect of eflornithine is through irreversible inhibition of ornithine decarboxylase leading to suppressed polyamine biosynthesis[66, 72]. The polyamines are necessary in the nucleic acid synthesis and contribute to the regulation of protein synthesis. Compared to human cells, the trypanosomes are more susceptible to the drug which is thought to be due to the slow turnover of the parasitic enzyme compared to human ornithine decarboxylase[66]. By inhibiting ornithine decarboxylase activity, eflornithine depletes the polyamines in trypanosomes, which brings the parasites into a static state that leave them to the host's immune attack[73]. Therefore, a sufficient active immune system is required to achieve a cure [74, 75]. Intravenous administration of eflornithine has proven to be relatively safe with 2-year cure rates reported to be 97 – 100% in either new or relapse patients (previously treated with melarsoprol) from Cote d'Ivoire, Congo and Zaire [76-80]. However, the main problem with eflornithine is the complicated mode of administration leading to logistical problems leaving numerous patients untreated. A more simplified mode of administration with eflornithine would potentially enable more patients to have access to treatment. Attempts to develop an oral treatment regimen with racemic eflornithine have so far been discouraging, probably due to inadequate bioavailability and possibly dose-limiting gastrointestinal side effects [81].

Pharmacokinetics and pharmacodynamics of eflornithine

Eflornithine elicits its pharmacological effect both in the hemolymphatic system and in the central nervous system (CNS). However, eflornithine is only administered once parasites have been detected in the central nervous system suggesting that the drug has to reach CNS to cure the established CNS infection[69]. For eflornithine, cerebrospinal fluid (CSF) concentrations have been used clinically as a surrogate for CNS exposure. Eflornithine CSF concentrations have been reported to be 10 – 50 % of those in plasma despite a negligible plasma protein binding [77, 81]. This concentration difference has been suggested to be a consequence of low permeability across the blood brain barrier. The major factor for efflux mechanism has been proposed to be driven by the cerebrospinal fluid bulk flow, based on CSF pharmacokinetic studies in the dog[82, 83]. However, the mechanism is not well characterized.

The eflornithine enantiomers have been shown to have different *in vitro* potency, with the L – enantiomer having a 20-fold higher affinity for human ornithine decarboxylase[5]. L – eflornithine also appears to be more potent in cultured *T.brucei* parasites (R.Brun, Swiss Tropical Institute, personal communication). The difference in potency therefore suggests that when eflornithine enantiomers are present in equimolar amounts it is primarily the L – form that elicits the trypanostatic effect.

The compound has a structurally similarity to an amino acid with a molecular weight of 182.2 g/mol (Figure 3). It is hydrophilic (logP = -2.31) and does not bind significantly to

plasma proteins[4, 84]. Regarding clinical pharmacokinetics, both volume of distribution and clearance are low with values of 0.2 – 0.8 L/kg and 1 – 2 mL/min/kg, respectively. The bioavailability has been reported to be between 50 and 100 percent. Both in man and in the rat, eflornithine is approximately 80% renally cleared and no metabolites have been found [4, 84, 85]. Despite the large difference in *in vitro* potency, no stereoselective pharmacokinetics has been published prior to the present thesis.
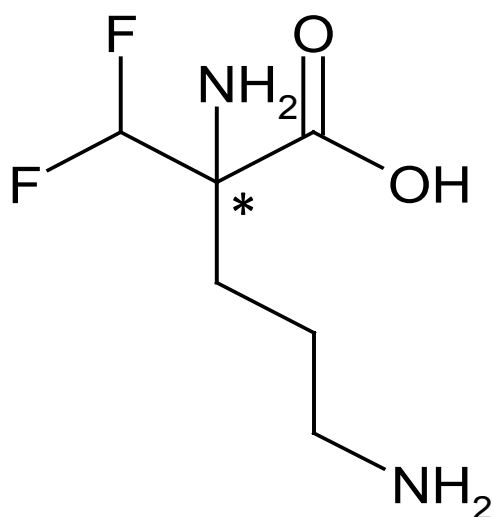

Figure 3. Structure of D,L-α-difluoromethylornithine. The chiral centre is marked by a star (*).

Determination of eflornithine enantiomers in biological matrices

Quantitation of drugs in biological matrices is the foundation of all experimental pharmacokinetic studies. A common way to determine drug concentrations is by the use of high performance liquid chromatography (HPLC) and UV – detection. However, for compounds without chromophores UV – detection cannot be applied. One way to address this problem is by derivatization meaning that a substrate will form a complex with the drug of interest and the resultant derivate can be detected with UV [86].

For chiral separation of compounds, a chiral stationary phase can be used for separation of the enantiomers [87]. Another option is derivatization with a chiral derivate to generate diastereomers [88]. The diastereomers can then be separated on columns not consisting of a chiral matrix. A third option is to use an achiral stationary phase and a chiral eluent.

For eflornithine there are a number of methods available for non-stereoselective determination [89-93], however only two methods are available for stereospecific determination. The first separation method was based on HPLC using L-proline/Copper

18

as a chiral eluent and also by gas chromatography on a Chirasil-Val as mono-N-perfluoroacyl ethyl ester derivates of the lactam. However, this method was primarily used for semipreparative resolution and not developed for determination for L – and D – eflornithine in biological matrices [94]. The second method available, was based on solid phase extraction and direct separation by liquid chromatography on a Chirobiotic TAG column with evaporative light-scattering detection [87]. This method was developed for the determination of L – and D – eflornithine in plasma and was validated for plasma determination according to appropriate guidelines [95]. However the limiting factor with this method is its long analytical time and inadequate sensitivity.

Pharmacokinetic data analysis

There are several ways to analyze pharmacokinetic data. The choice of pharmacokinetic data analysis depends primarily on the purpose of the analysis. The two most common ways to analyze data are by non-compartmental analysis (NCA) or compartmental analysis.

Using non-compartmental analysis one does not make assumptions regarding the shape of the plasma-concentration time curve, however it assumes that elimination occurs from the sampling compartment. With this method, the area under the curve (AUC) is used to estimate the pharmacokinetic parameters. The main disadvantage is that it requires frequent sampling from each individual [1].

Compartmental analysis treats the body as being composed of a number of pharmacokinetically distinct compartments. The number of compartments in a model is empirically determined based on the plasma concentration time profile. When using this method, assumptions need to be made regarding the shape of the curve. The compartmental modeling approach can provide an empirical assessment of changes in physiological processes such as membrane transport or metabolism without thorough mechanistic investigations[97]. The primary advantage of the compartmental modeling approach is that allows the possibility to simulate concentration time profiles for other dose levels and frequencies. Ideally the model should be mechanistic in nature, which facilitates extrapolation from the experimental condition under which the model was built. Sometimes, a mechanistic model is not possible and an empirical model can be used that adequately describes the data, assuming that it can be used for the specific purpose of the modeling [98]. In a sense, mechanistic or empirical, all models are more or less wrong but some are useful [99].

Non-linear mixed effects modeling

Pharmacokinetic parameters can vary to a large extent between individuals. The traditional way to estimate the inter-individual variability is to use a two-stage approach where a model is fitted to each individual and thereafter inter-individual variability is calculated [100]. The problem with this method is that it requires frequent sampling from

all individuals and sometimes the same structural model cannot be fitted to all individuals, which can cause problems when calculating between subject variability. A two-stage approach can also lead to overestimation of the interindividual variability as this method does not discriminate between random residual variability (unexplained variability) and variability in pharmacokinetic parameters. Another approach is to use non-linear mixed effects modeling, where a minimum of two levels of variability can be identified and separated. The first level handles random residual variability which is the unexplained variability such as measurement errors and model misspecification. The second level can explain between- and within- subject variability of parameters. This method also includes structural parameters which are constant for all individuals (referred to as fixed effects parameters). In non-linear mixed effects modeling, the model is fitted to all observations simultaneously allowing discrepancy between unexplained variability and between-subject variability [100]. This method also allows the possibility to implement covariates such as body weight, age, sex, dose levels, renal function and drug-drug interactions.

The general workflow for the population based model building process (and in a sense all types of model building processes), after visual exploration of the data, is to first find an adequate structural model, which can explain the population mean data. Next, variability (random residual and between subject variability) is identified and quantified. In addition, identification of possible correlations between model parameters needs to be evaluated. Thereafter, a covariate model, aiming to find relationships between model parameters and measured covariates can be introduced. This is the general workflow of the modeling process that is most commonly used in population based PK/PD [101]. During each step, the model is fitted to the data and evaluated using appropriate diagnostic tools. Once a final model has been determined, it should be evaluated with methods such as visual predictive checks [102] and bootstrap estimation.

Non-linear mixed effects modeling is primarily used in clinical studies, where variability of the pharmacokinetic parameters are in general higher compared to preclinical *in vivo* studies, but it has also advantages in preclinical *in vivo* studies [103, 104]. It has also been shown to be useful for detection of nonlinear pharmacokinetics [105].

Aims of the Thesis

This thesis aimed to address two issues, namely, prediction of drug tissue to plasma concentration ratios and stereoselective pharmacokinetics. For the stereoselective pharmacokinetics, the trypanostatic drug eflornithine was taken as a case example.

Specifically the aims were:

- To develop a general method to predict drug specific tissue-plasma concentration ratios, based on a measured volume of distribution in combination with compound lipophilicity

- To develop a method for determination of eflornithine enantiomers in plasma

- To investigate the pharmacokinetics of L- and D- eflornithine, in the rat, after single oral and intravenous administration of racemic eflornithine

- To characterize the stereoselective pharmacokinetics of eflornithine in late-stage HAT patients receiving oral eflornithine, and its possible clinical consequences

Materials and Methods

Litterature collection and study designs

Paper I

The general method for prediction of tissue distribution was generated upon literature data for a wide range of drug compounds. *In vivo* determined Kp values were collected, according to criteria similar to those presented by Björkman [106], and a value for volumes of distribution in the same species were collected. In addition, physicochemical properties such as logP and pKa, were collected, from the database ChemID or when not found calculated using Pallas 3.2.1.4 (CompuDrug International Inc., CA, USA).

Data for a total of 71 compounds were collected that fulfilled the criteria. For 52 of these compounds it was possible to obtain a volume of distribution in the same species. The dataset was divided into two subsets, one for acids and zwitterions and another for bases and neutrals. Each these two sets were then subdivided into a training set and a test set. The test set for acids and zwitterions consisted of 7 acids and 2 zwitterions and the test set for bases and neutrals consisted of 10 bases and 3 neutrals. The remaining drug compounds constituted the two training sets.

Paper II

This was a pilot study to investigate the stereoselective pharmacokinetics of eflornithine, after single oral and intravenous dose to the rat. Due to limited sensitivity of the stereoselective bioanalytical method available, a combination of stereospecific and nonstereospecific quantitation was used. The oral doses corresponded to 750 – 3000 mg/kg bodyweight, administered by gavage and intravenous short term-infusions (3 minutes) ranging from 375 – 1000 mg/kg bodyweight (Table 1). For rats receiving eflornithine intravenously arterial blood samples were drawn and for rats receiving eflornithine orally intravenous blood samples were collected.

Table 1. Experimental design for paper II

Route	Racemic dose (mg/kg bodyweight)	No. of rats for chiral analysis (1–3 plasma samples/rat)	No. of rats for non-stereoselective analysis (8-16 plasma samples/rat)
Oral	750	10	4
Oral	1500	9	4
Oral	2000	7	4
Oral	3000	10	4
Intravenous	375	5	4
Intravenous	1000	5	3

Paper III

For further investigations of the stereoselective pharmacokinetics of eflornithine a more sensitive method of analysis was required. The validation of the stereoselective determination of eflornithine was setup according to the FDA guidelines [95].

Paper IV

To further explore the nonlinear and enantioselective absorption of eflornithine enantiomers, another study was conducted at more appropriate dose levels employing the improved assay. However, to possibly generate more data regarding the mechanism of absorption a wide dose range was applied.

Oral doses were administered by gavage at a volume of 10 mL/kg bodyweight for each dose level of 40 – 3000 mg/kg bodyweight of racemic eflornithine. Intravenous infusions for 60 – 400 minutes were done to resemble the plasma concentration time profile after oral administration. The dose levels ranged from 100 – 2700 mg/kg bodyweight of racemic eflornithine. The intravenous volume administered was 10 mL/kg bodyweight over a pre-set time interval (Table 2).

During infusions, the rats were connected to a balancing arm and swivel, ensuring rats were freely moving. After the end of infusion, rats were disconnected from the balancing arm. Independent on route of administration, serial arterial blood samples were collected for determination of L – and D - eflornithine. For a number of rats, feces were collected to investigate whether the differing fraction absorbed was a consequence of presystemic metabolism. This study also included Caco-2 cell experiments at donor enantiomeric concentrations of 0.75 and 12.5 mM (added as a racemate). To investigate whether P-gp was involved, incubations were done in the presence of GF120918 (10 μM) at incubations of 0.75 mM for each enantiomer. Incubations were performed at pH 7.4 at both the apical and basolateral side.

Table 2. Experimental design for paper IV

Route of administration	Racemic dose (mg/kg of bodyweight)	Length of infusion (min)	No. of rats
Intravenous	100	60	5
Intravenous	550	160 - 163	5
Intravenous	2700	400	5
Oral	40	-	5
Oral	150	-	5
Oral	400	-	6
Oral	1200	-	5
Oral	3000	-	5

Paper V
Based on the preclinical findings it was reasoned appropriate to reanalyze the separate eflornithine enantiomers in patients with late-stage *T.b.gambiense* sleeping sickness treated with oral eflornithine (100 or 125 mg/kg) every 6th hour for 14 days from a previously published study [81]. The sampling schedules for pharmacokinetics and CSF were identical for both study arms. A total of 14 blood samples were collected from all patients before treatment and before the second dose on day 10 and frequent blood samples following the last day of dose. CSF samples (3 ml) collected at diagnosis, 5 min before the second application on day 10, and 5 min before the last dose on day 15.

To ensure that eflornithine enantiomers had not been degraded, the sum of the determined L – and D – eflornithine plasma concentrations were compared to previously reported total concentrations (the sum of L – and D – eflornithine).

A population pharmacokinetic model was fitted to the plasma concentration time data. The association between the probability of cure and drug exposure, CSF concentrations (average days 10 and 15), plasma Css,min (average 6 hours post-dose) and AUC in a dosing interval, was explored by logistic regression against L – and total (D+L) eflornithine.

Animals and animal surgery

Animals

Papers **II** and **IV** were based on pharmacokinetic studies in the laboratory rat. Male Sprague-Dawley rats (260 – 365 grams) (B&K Universal AB, Sollentuna, Sweden for paper II and Charles River, Germany for paper IV) were allowed to acclimatize, at a certified animal facility, for 5 – 10 days prior to surgery. The animals were housed under controlled environmental conditions (12-h light-dark cycle at 25 to 27°C and 60 to 65% humidity). Four rats were kept in each cage prior to surgery and thereafter kept separately. Food (B&K Feeds, Harlan, USA) and tap water were available *ad libitum* prior to and after surgery. The studies were approved by the Ethics Committee for Animal Experiments, Göteborg, Sweden (255/2005).

Animal surgery

The animals were anesthetized by inhalation of isoflurane (2.9 to 3.7% in air). The left jugular vein was catheterized using MRE040 1.02-mm-outer-diameter (OD), 0.64-mm-inner-diameter (ID) tubing and the right carotid artery were catheterized using PE-50 0.96-mm OD, 0.58-mm-ID tubing (AgnThos, Lidingö, Sweden), prefilled with 100 IU/ml of heparin (Leo Pharma) in saline solution. Both catheters were tunnelled subcutaneously to emerge at the back of the neck. Catheters were kept patent with heparinized saline solution (20 IU/ml) between sampling to prevent blood clotting. All animals were allowed to recover for at least 16 h after surgery.

Eflornithine used in studies

Racemic eflornithine hydrochloride (DFMO*2HCl) used throughout paper **II – V,** was kindly donated by WHO/TDR (Geneva, Switzerland). L – eflornithine and D – eflornithine enantiomers (2 mg) were synthesized by Lipitek International Inc. (San Antonio, Texas, USA).

Analytical procedure

For **papers II – V** the LC system consisted of a 48-well plate Prospekt 2 autoinjector (SparkHolland, Emmen, Holland), two interconnected Schimadzu LC10AD pumps and a Schimadzu SPD 10-A UV-VIS detector (Schimadzu, Kyoto, Japan). Eflornithine separation was performed on Chrolomolith Performance columns (RP-18e 100 mm × 4.6 mm I.D.) protected by a Chromolith Guard RP-18e column (10 mm × 4.6 mm I.D.) (VWR International, Darmstadt, Germany).

Non-stereoselective determination in paper II was analyzed based on a published method [92]. L – and D – eflornithine in paper II was analyzed with a previously developed method in the same laboratory where it was developed [87]. For paper IV and V, the method developed in paper III was used.

Software

In paper **I**, the regression analysis, for obtaining correlations between tissue to muscle was analyzed using SPSS (SPSS Inc. Chicago, Illinois, USA) [107]. For discrimination between hierarchical models a F – test was used [108].

Chromatographic data acquisition for paper **II – V** was performed using Chromatographic Station for Windows version 1.2.3 (Dataapex, Prague, The Czech Republic).

In papers **II, IV, V**, pharmacokinetic data was modeled by means of nonlinear mixed-effect modeling using maximum likelihood estimation in the computer program NONMEM V or VI (Icon Development Solutions, Elliot City, MD, USA) [109]. Pharmacokinetic data was analysed using the first-order conditional estimation with interaction (FOCE INTER). In paper **V** logistic regression analyses were done by the FOCE and the LAPLACE option.

Graphical diagnostics and parameter estimates were evaluated using the software Census version 1.0 [110]. For papers **IV** and **V** bootstrap estimates derived from nonparametric bootstrap and visual predictive checks were also used as diagnostic tools using the software Pearl Speaks NONMEM [102, 111].

In paper **IV**, deconvolution methodology and non-compartmental analysis was conducted using the software WinNonlin 5.2 (Pharsight, Ca., USA).

Data analysis

Paper I
The general method for prediction of tissue Kp values was developed requiring an *in vivo* measured volume of distribution. The model was built upon the concept that partitioning into non-adipose tissues correlate to muscle partitioning [8, 106]. The Kp values were log-transformed prior to regression:

$$\log Kp_{tissue} = a_{tissue} \bullet \log Kp_{muscle} + intercept_{tissue} \qquad \textbf{[1]}$$

where a_{tissue} is the slope for tissue

Drug lipophilicity was evaluated as a covariate to improve this correlation:

$$\log Kp_{tissue} = a_{tissue} \bullet \log Kp_{muscle} + b_{tissue} \bullet \log X_{drug} + intercept_{tissue} \quad \textbf{[2]}$$

Where LogX$_{drug}$ is the compound-specific lipophilicity (LogP, LogD, LogK$_{7.4}$). If the LogD or LogK$_{7.4}$ value was unavailable it was calculated according to previous methodologies [9, 112]. A F-test was used to discriminate whether drug lipophilicity should be included or not (eq. 1 and 2) [108].

According to theory a measured volume at steady state (Vss), will equal plasma and the sum apparent volume for each tissue [12, 113]:

$$Vss = V_{plasma} + \sum_{i=1}^{n} V_{tissue\,i} \bullet Kp_{tissue\,i} \qquad [3]$$

Where V$_{plasma}$ is the plasma volume, V$_{tissue,I}$ is the volume for each tissue and Kp$_{tissue,i}$ is the drug specific tissue-to-plasma concentration ratio.

By insertion of tissue regression equations (eq 1 and 2) into equation 3 correspond to:

$$Vss = V_{plasma} + \sum_{i=1}^{n} V_{tissue_i} \bullet 10^{a_{tissue,i} \bullet Kp_{muscle} + intercept_{tissue,i}}$$

$$+ \sum_{j=1}^{n} V_{tissue\,j} \bullet 10^{a_{tissue,j} \bullet Kp_{muscle} + b_{tissue,j} \bullet \log X_{drug} + intercept_{tissue,j}}$$

$$[4]$$

Where i and j represent tissues for which a lipophilicity descriptor is excluded or included in the Kp$_{tissue}$ to Kp$_{muscle}$ model, respectively.

Equation 4 represents the final prediction model which was used for prediction of drug specific tissue Kp values. Physiological volumes corresponded to those in the rat [114]. By inserting Vss, physiological volumes of each tissue and obtained correlations between a specific tissue to muscle (eq 1 or 2) an equation was generated were only one variable was unknown: Kp-muscle. Equation 4 could then be iteratively solved to obtain Kp-muscle and therefore indirectly the other Kp-tissue values as well.

In paper II, the limiting factor was the inadequate sensitivity for the stereospecific bioanalysis at hand. To stabilize the sparse enantiomeric data rich D,L – eflornithine concentration data were modeled simultaneously. In the modeling process D,L–eflornithine concentrations were set to be the sum of D – and L – eflornithine concentrations. The intravenous data was described with a two-compartment model. The selected structural model, with its estimated parameters after intravenous dosing were then used as fixed parameters to model the oral data.

The delay in absorption was modeled with a transit compartment model, using a Stirling approximation for estimating the number of transit compartment prior to reaching the dose compartment [115-117].
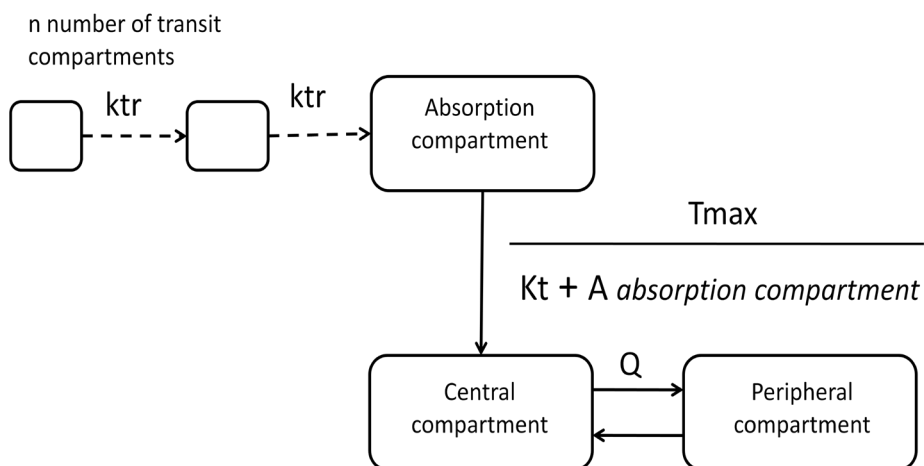

Figure 3. Structural model for L – and D – eflornithine after intravenous and oral administration. The transit compartment absorption consisted of a number of transit compartments (n) and the transit compartment rate (ktr) delivering the drug to the absorption compartment. The transfer of drug from the absorption compartment to the central compartment was modeled with a Michaelis-Menten type function, using the parameters Tmax, Kt, and the amount of drug in the absorption compartment. Intercompartmental clearance (Q) and the volume of the central and peripheral compartments were fixed from the intravenous data.

In **paper III** standard statistical methods, relevant for bioanalytical method development, were used [118].

In **paper IV,** the intravenous data was modeled by compartmental analysis and oral data was analyzed by noncompartmental analysis (NCA) and deconvolution methodology.

NCA analysis was performed using the log-linear trapezoidal method with extrapolation to infinity by C_{pred}/λ_Z , for each individual animal up to the last sampling point. The terminal elimination half-life was estimated by log-linear regression of 3 to 4 observed concentrations. To investigate the gastrointestinal absorption, deconvolution methodology was applied using WinNonlin 5.2 [96].

In **paper V** a two-compartment model, with first-order input, with lag-time and first-order elimination was used. Potential covariates (dose level, bodyweight, age, gender, concomitant medication, hemoglobin levels) for plasma pharmacokinetics, were visually explored and later on added as linear or categorical covariates. Inclusion of covariates was achieved by using the log likelihood ratio where the difference in the OFV between the full and reduced models was asymptotically chi-square distributed. Decreases in the OFV

of 3.84 and 6.63 between two nested models (1 degree of freedom) were considered to indicate a statistically superior model ($P < 0.05$ and $P < 0.01$, respectively).

The area under the plasma concentration curve for a dosing interval of six hours (AUCτ) was individually calculated from the model-based CL/F as

$$AUC_\tau = Dose / (CL/F)$$

Binary cure data in paper IV was analysed using a probability function. The probability of cure was modelled by logistic regression versus observed steady state CSF (average concentration from day 10 and 15), the observed average through plasma concentration Css,min at steady state (average concentration 6 hours after dose administration, n=3) and AUC$_\tau$.

$$P(Cure) = \frac{e^{\wedge}(a + b \times C)}{1 + e^{\wedge}(a + b \times C)}$$

where *a* is an intercept and *b* is a measure how steeply the probability changes with an increase in eflornithine concentration or exposure (C).

Results and Discussion

Prediction of drug tissue to plasma concentration ratios – Paper I

Correlations between tissues, were generally improved by separating the training set into two groups according to their protolytic properties compared to when fitting all compounds together, which also agreed with previous findings[106]. For bases and neutrals, a significant improved correlation (F-test, $p < 0.05$) was obtained when including compound lipophilicity for brain, heart, lung and adipose tissue (Table 3). For acids and zwitterions, the correlation between brain, heart, liver, kidney and adipose with muscle was significantly improved ($p < 0.05$, Table 3) when incorporating compound lipophilicity as covariate.

The generated model could reasonable well predict Kp values and performed better than the Poulin and Theil approach [8, 11] (Table 3, Figure 4). The empirical method to predict tissue-to-plasma concentration ratios performed reasonably well with experimentally determined values, particularly for non-eliminating tissues ($r^2 = 0.81$) with 72% and 87% being within a factor of ± 2 and ± 3, respectively. This was an improvement in comparison to the Poulin and Theil approach, for which 53% and 66% were within a factor ± 2 and ± 3, respectively.

The general method for prediction of drug Kp values was based on a large number of experimentally determined Kp values. The reliability of experimentally determined Kp values has previously been discussed and it has been observed that *in vivo* determined tissue partitioning can differ for the same compound in the same specie by a factor of 3 between laboratories [8, 9, 13, 14]. Considering this it becomes obvious that predictions may deviate from the experimental values up to 3-fold due to inaccurate experimental values. Liver Kp values were less accurately predicted, compared to non-eliminating tissues. Two possible reasons for this lack of agreement were probably due to the presence of transporters in the liver and the extraction across eliminating organs [119, 120].

Table 3. Parameter estimates obtained when regressing LogKp tissue to Log Kp muscle and compound lipophilicity ($logX_{drug}$)

Organ/tissue	n	a (SE)• $LogKp_{drug}$	b (SE)• $LogX_{drug}$	Intercept (SE)	r^2
Acids and zwitterions					
Brain	9	0.620 (0.281)	0.255 (0.049)"	-0.442 (0.116)	0.83**
Heart	17	0.845 (0.051)	0.033 (0.008)"	0.140 (0.025)	0.97**
Lung	20	0.790 (0.095)		0.166 (0.055)	0.80
Gut	14	0.520 (0.209)		0.206 (0.136)	0.34
Liver	13	0.484 (0.213)	0.074 (0.034)"	0.382 (0.129)	0.69*
Kidney	13	0.337 (0.096)	-0.070 (0.015)"	0.524 (0.058)	0.69**
Bone	3	0.817 (0.155)		-0.042 (0.106)	0.97
Skin	12	0.663 (0.167)		0.165 (0.081)	0.61
Adipose	9	0.897 (0.166)	0.265 (0.021)#	0.084 (0.056)	0.97**
Bases and neutrals					
Brain	20	0.745 (0.162)	0.177 (0.051)"	-0.167 (0.107)	0.75**
Heart	26	0.954 (0.079)	0.168 (0.032)"	-0.023 (0.079)	0.89**
Lung	27	0.431 (0.161)	0.371 (0.060)+	-0.129 (0.182)	0.83**
Gut	16	1.049 (0.090)		0.368 (0.065)	0.92
Liver	12	1.226 (0.261)		0.779 (0.159)	0.69
Kidney	18	0.843 (0.135)		0.732 (0.083)	0.71
Bone	8	0.911 (0.044)		-0.113 (0.036)	0.99
Skin	14	0.771 (0.111)		-0.060 (0.083)	0.81
Adipose	17	1.277 (0.208)	0.336 (0.120) #	-0.249 (0.179)	0.84*

The general equation for describing the correlation was:

Log Kptissue = a_{tissue}•logKpmuscle + b_{tissue}•logXdrug + intercept

* = significant better correlation (F-test, $p < 0.05$) by incorporating either LogP,LogD or LogK7.4

** = significant better correlation (F-test, $p < 0.01$) by incorporating either LogP, LogD or LogK7.4

" = LogD was used, based on the SSR value

+ = logP was used, based on the SSR value
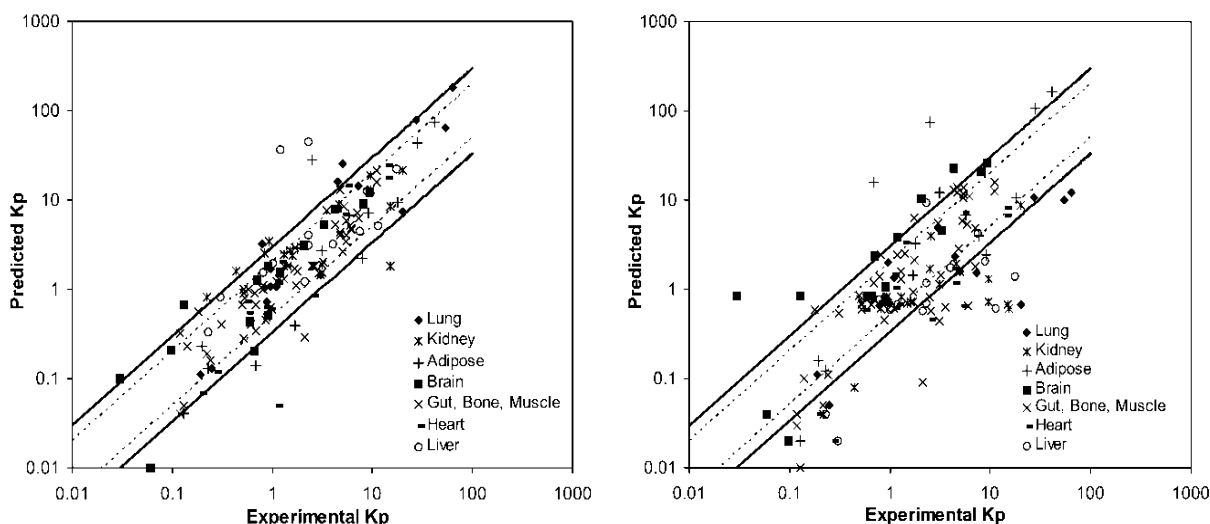
= logK7.4 was used, based on the SSR value

Figure 4. Predicted Kp values versus experimentally determined values in the test set according to tissue. The left graph corresponds to predictions based on a measured volume of distribution and lipophiliticity. The right graph shows predictions using a tissue composition based (TCB) approach. The dashed and solid lines correspond to a factor of 2 and 3, respectively, on either side of the line of unity.

Table 4. Summary of the Kp prediction accuracy by the presented empirical method and a previously published tissue composition based (TCB) approach.

	Percentage of ratios between predicted to experimental Kp values being within a factor of:				Mean (± SD) Predicted to Experimental Kp Ratio
	< 2	< 3	< 4	< 10	
All compounds (n= 148)					
Empirical method	72	85	92	97	1.71 ± 3.07
Using a TCB approach	49	64	76	91	1.64 ± 3.86
All compounds excluding eliminating organs (n= 118)					
Empirical method	72	87	92	98	1.35 ± 1.29
Using a TCB approach	53	66	80	94	1.92 ± 4.27

33

Overall this method performed reasonably well although it requires an accurate determined volume of distribution at steady state since it will affect all Kp values. For compounds undergoing extensive enterohepatic recirculation it will exhibit apparently high estimates of volumes of distribution despite low partitioning into tissue which will lead to overpredicted Kp values.

The presented model was a general method to predict tissue distribution for a wide range of compounds. This model may aid the use of physiologically based pharmacokinetic (PBPK) model simulations when available *in vitro* methods fail to give reasonable estimates of Kp values. The method can also have applicability when drug experimental Kp-muscle has been determined for a particular compound. The experimental Kp-muscle value can then be used to predict other tissue Kp values. Comparing model predicted Kp values to experimental determined values, may give information on whether there is a large drug accumulation (*i.e.* high Kp-value) in a specific tissue compared to what is expected.

The stereoselective pharmacokinetics of eflornithine in the rat – Paper II

This pilot study, conducted in the rat, displayed a large enantiomeric difference in exposure after oral administration with the L – form having approximately 50 % lower exposure compared to the D – enantiomer. After intravenous administration, L – and D – eflornithine plasma concentrations were comparable up to the last sampling time point.

Simultaneously fitting L – and D – eflornithine concentrations with the D,L – eflornithine concentrations stabilized the data and provided more reliable estimates compared to when fitting enantiomers separately. The intravenous data was described with a two-compartment model with linear elimination. Clearance and central volume of distribution could be estimated separately for L – and D – eflornithine. Intercompartment clearance (Q) and peripheral volumes were estimated as being the same for both enantiomers. Marginal difference was observed in clearance with mean values for L – and D – eflornithine of 14.5 and 12.6 ml/min/kg bodyweight, respectively.
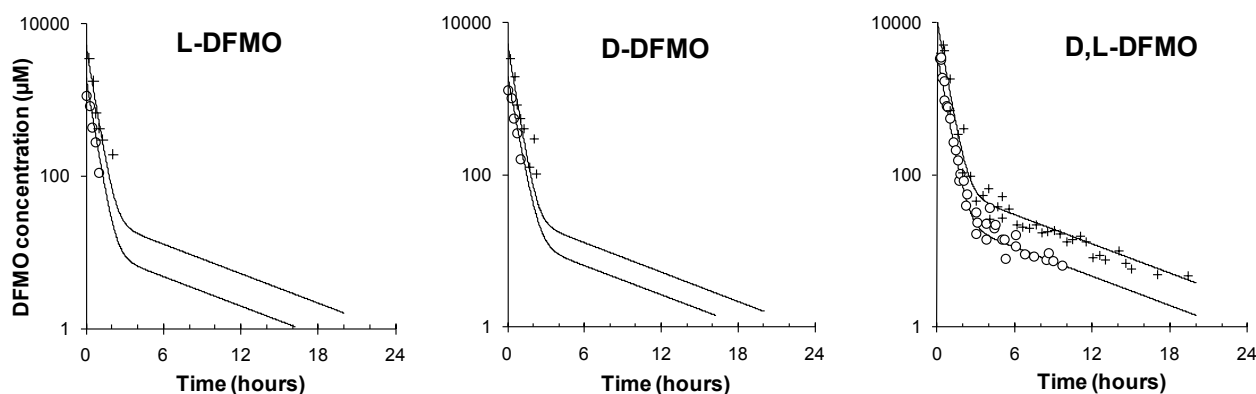
Figure 5. Experimental values for L −,D − and D,L − eflornithine (DFMO) after intravenous administration of 375 (O) and 1000 (+) mg/kg bodyweight of racemic eflornithine to rats (n=17). D,L − eflornithine (DFMO) corresponds to concentrations determined with a non-stereoselective assay. The black solid lines represent the population predicted values, for the corresponding dose levels and enantiomers.

The oral data indicated a nonlinear absorption mechanism. Oral data was described with a transit model to mimic the delay in absorption[115]. In the absorption compartment, the transfer of drug to the central compartment was described with a Michaelis-Menten (hyperbola) type function.

The population mean bioavailability, in the dose range of 750 to 2000 mg/kg bw, were 41 % (95% CI: 35, 46%) and 62 % (95% CI: 51, 74 %). At the highest dose level (3000 mg/kg bw) a small but abrupt increase in bioavailability was observed. This slight increase in bioavailability was estimated as a categorical parameter for both L − and D − eflornithine which gave a significant drop in the objective function value (p <0.01, ΔOFV -11.4). Estimated bioavailabilities at the 3000 mg/kg bw level corresponded to 47% (95% CI: 40, 54 %) and 83 % (95% CI: 72, 93%), for L − and D − eflornithine respectively. The mechanistic reason for this slight increase in bioavailability could however not be explained. The absorption model suggested an active uptake across the gastrointestinal tract but was contradicted with the small but abrupt increase in bioavailability

This study was based on the simultaneous modeling of sparse enantiomeric data combined with rich non-stereoselective (the sum of L − and D − DFMO) data. Eflornithine enantiomers exhibited enantioselective bioavailability which was suggested to be caused by stereoselective absorption across the gastrointestinal tract. These findings gave a suggestion why previous attempts to develop an oral treatment had failed and required further investigation.
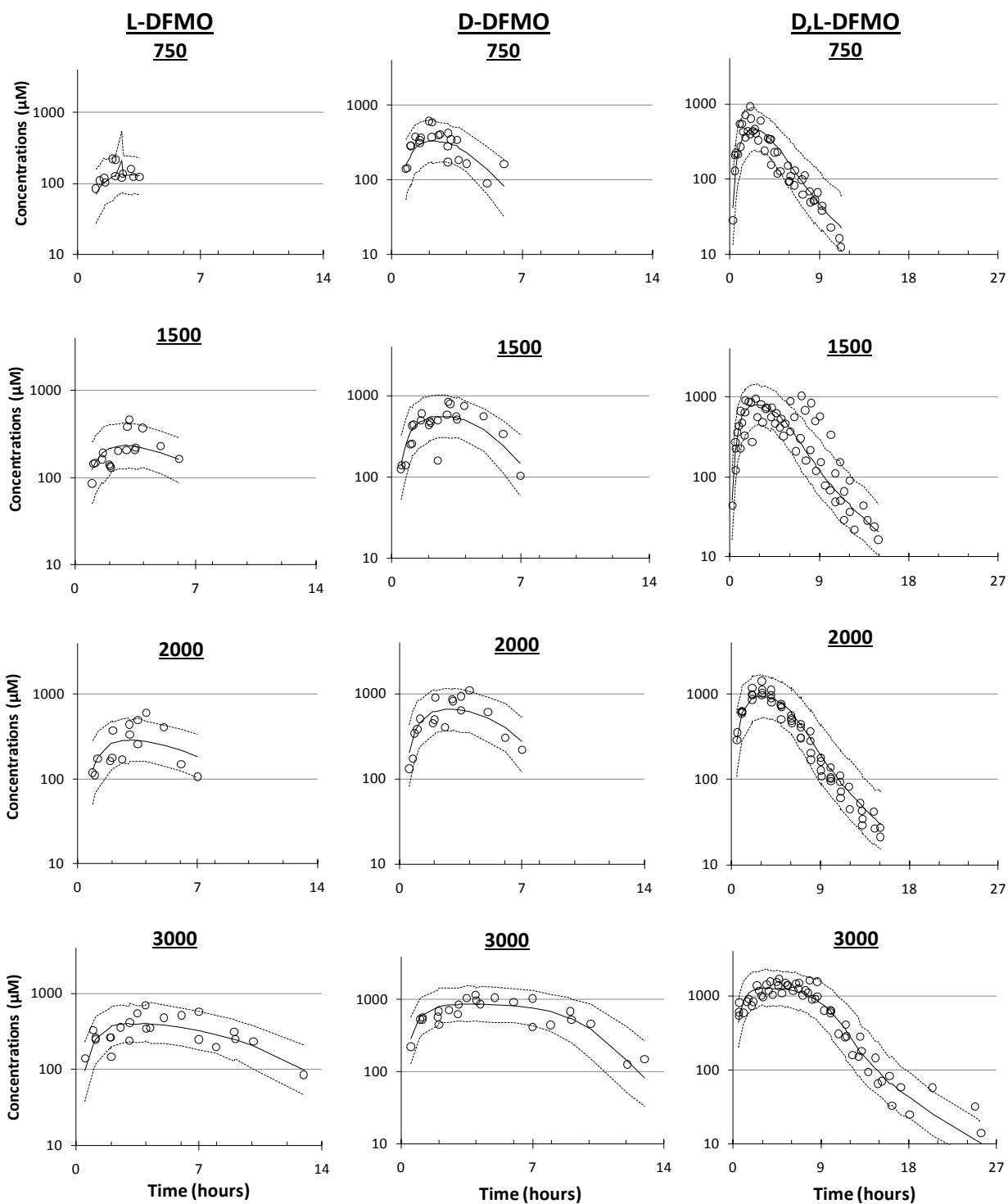
Figure 6. A visual predictive check of the final models ability to predict the observations in an oral racemic dose range of 750 – 3000 mg/kg bodyweight, administered to the rat. Intravenous disposition parameters were fixed and obtained from the intravenous data. The study was replicated 1000 times. Circles represent observed values and the dashed lines correspond to the 95% Confidence Intervals around the median predicted concentrations (black solid line). The predictive check was divided into L – (left column), D – (middle column) and D,L – DFMO (right column). Rows were divided into racemic oral dose levels (mg/kg bodyweight) administered to the rat.

Determination of eflornithine enantiomers in plasma – Paper III

Separation of L – and D – eflornithine enantiomers was achieved by the use of precolumn derivatization with *o*-phthalaldehyde and *N*-acetyl-L-cysteine on two serially connected monolith C-18 columns. Enantioseparation and sequence of elution was confirmed by injecting plasma or water to which either L – or D –eflornithine was spiked (Figure 7 B and C). At the highest calibration standard (1250 µM) the resolution (Rs) was 1.1 and the separation factor α was 1.2. Peak area against corresponding nominal concentration with linear regression and $1/x^2$ weighting was selected as the most appropriate regression model for the calibration curve. The coefficient of determination over five days of validation (r^2) was $> 0.993 \pm 0.005$ (mean ± SD, n=5) for both enantiomers.

Recovery was reproducible over three days and independent upon concentration (Table 5.) with total assay precision, for each QC level and enantiomer, between 7.9 and 14.3% (n=5 at each QC level and enantiomer for each of the three analytical runs). The Lower Limit of Quantitation (LLOQ) was set to 1.5 µM at which precision was 14.9 % and 9.9% and accuracy -11.4% and -0.4% (n=8) for L – and D – eflornithine, respectively. Accuracy and precision for QC samples were within recommended guidelines (Table 5) [118].

None of the pharmaceuticals evaluated interfered with L – and D – eflornithine and blank plasma from six healthy donors did not chromatographically interfere at the retention times of L – and D – eflornithine.

Table 5. Accuracy, intra- and inter- assay precision, and extraction recovery for the determination of L – and D – eflornithine in 75 µL human plasma.

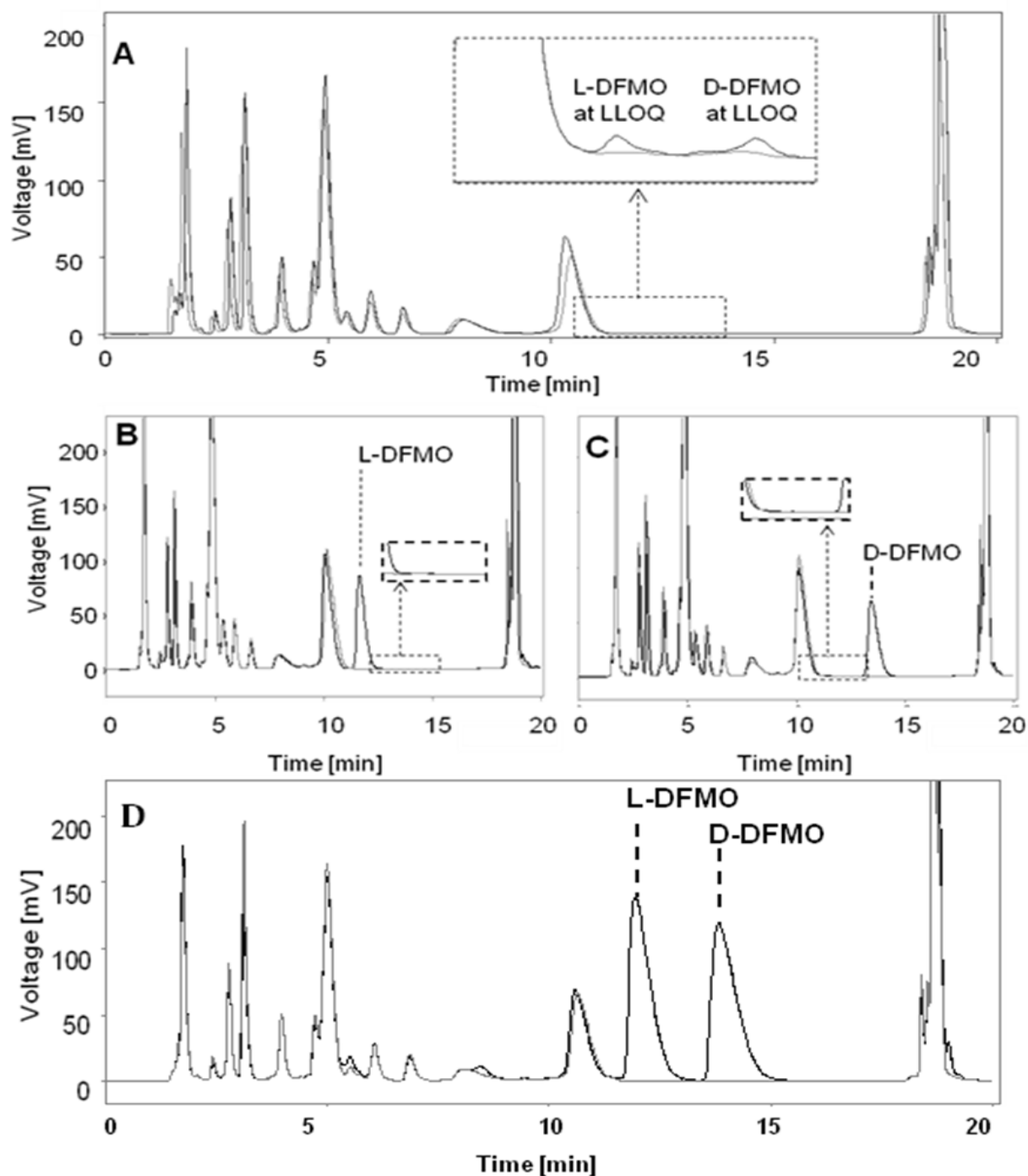|	QC 1 (3 µM)		QC 2 (400 µM)		QC 3 (1000 µM)	
	L-DFMO	D-DFMO	L-DFMO	D-DFMO	L-DFMO	D-DFMO
Experimental concentration (mean)	2.8	2.9	373	383	1047	1078
Within-day precision (%), n=25	9.7	7.6	4.9	4.8	6.9	6.8
Between-day precision (%), n=5	8.4	2.3	4.0	5.1	2.0	3.7
Total assay precision (%)	13	7.9	6.3	7.0	7.2	7.7
Accuracy (%)	-7.9	-4.2	-6.7	-4.3	5.5	9.0
Recovery (mean %)	72	71	66	67	72	73

Figure 7. A) Chromatogram of L – and D – eflornithine at LLOQ (black chromatogram) and blank plasma (grey chromatogram). B) Chromatogram of L – eflornithine (black chromatogram), at a nominal concentration of 450 µM. The grey chromatogram corresponds to blank plasma. C) Plasma spiked with the separate D – enantiomer at a concentration of 390 µM and blank plasma (grey chromatogram). D) Plasma spiked with a racemic mixture corresponding to 1250 µM of L – and D – DFMO.

The method for determination eflornithine enantiomers was based on an established precolumn derivatisation method used for amino acid enantiomer determination [88]. The optically active thiol N-acetyl-L-cysteine, in the presence of o-phtalaldehyde will react with the primary amine to generate diastereomers. For eflornithine there are two amines that might potentially react with the active derivate. The structure of formed diastereomers could therefore not be proposed. However, during method development, no other diastereomers were detected, except those displayed in the chromatograms. Taken together with that response was linear, there were no difference in slopes between L – and D – eflornithine in the calibration curve, and no other peaks detected when analyzing the separate enantiomers it was concluded that this method was reliable for determination of L – and D – eflornithine.

Overall, this method of bioanalysis was more than 15-fold more sensitive compared to the previous method available for quantitation of eflornithine enantiomers in plasma and requiring a 13-fold lower sampling volume [87]. It was found to be accurate, reproducible and as far could be ascertained, selective. This method allowed further studies of the stereoselective pharmacokinetics of eflornithine.

Stereoselective pharmacokinetics in the rat and bidirectional permeabilities in Caco-2 cells – Paper IV

After intravenous administration clearance was linear over the entire dose range and did not differ for the enantiomers (Figure 8). Intercompartmental clearance exhibited a trend towards a decrease at escalating dose levels. However due to the shorter duration of sampling times at lower dose levels it was not included as a covariate. No trend in central or peripheral volume of distribution was observed over the dose range studied. Based on compartmental analysis, clearance for L – and D – eflornithine were 3.31 (95%CI: 3.05, 3.55) and 3.18 (95%CI: 2.94, 3.42) mL/min, respectively, for a typical rat weight of 338.4 grams.
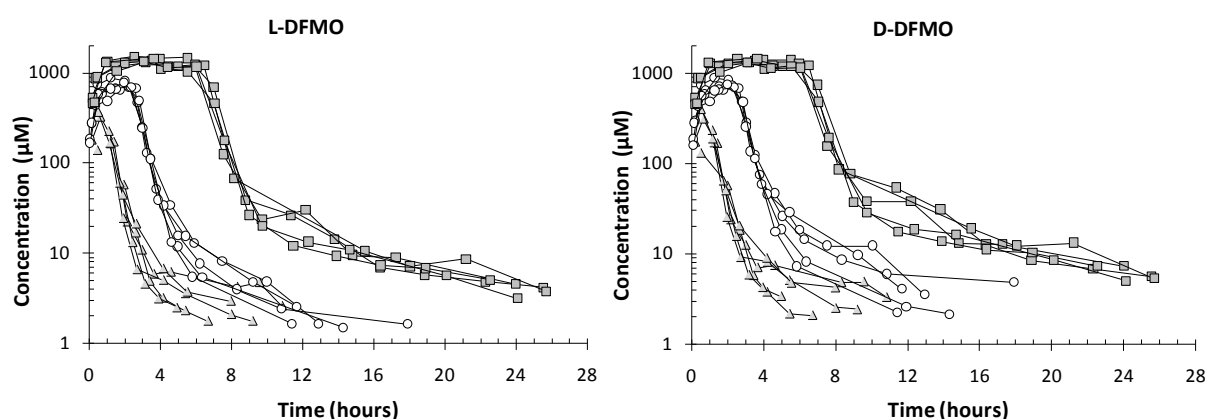

Figure 8. Experimental values of L – and D – eflornithine after intravenous administration of racemic eflornithine of 100 (Δ), 550 (O) and 2700 (□) mg/kg bodyweight. Infusion times for the escalating dose levels were 1 hour, 2 hours, 40 minutes and 6 hours, 40 minutes. Individual observations are interconnected by thin lines.

In agreement with the results in paper II, eflornithine displayed enantioselective bioavailability (Table 6). It was concluded that the differing bioavailabilities was not caused by presystemic metabolism. This was based on the finding that fecal D:L concentration ratio after oral administration, was 0.49 ± 0.03 (SE) which was the inverse to that observed in plasma.
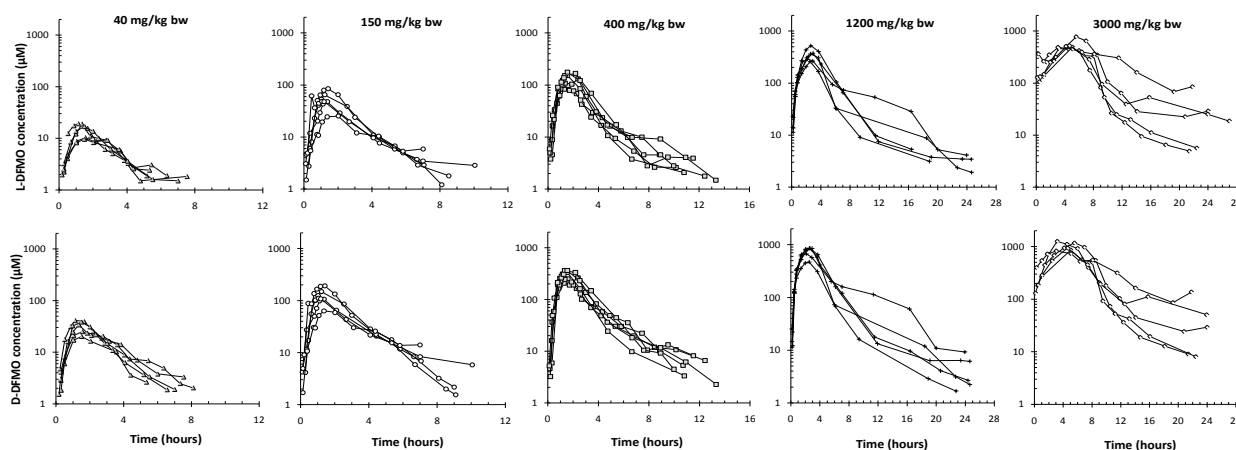

Figure 9. Experimental values of L – (upper row) and D – eflornithine (lower row) after oral administration of racemic eflornithine of 40, 150, 400, 1200 and 3000 mg/kg bodyweight.

Table 6. Non-compartmental analysis of L – and D – eflornithine pharmacokinetics, after single oral racemic dose to the rat.

Racemic dose level (mg/kg bw)	N	Cmax/Dose (L)	Tmax (hours)	$AUC_{0-\infty}$/Dose (min/L)	F (%)
L-eflornithine					
40	5	0.53 (0.38, 0.74)	1.4 (1.2, 1.6)	96 (85, 108)	32 (28, 36)
150	5	0.49 (0.33, 0.77)	1.2 (0.67, 2.0)	80 (63, 102)	26 (21, 34)
400	6	0.49 (0.38, 0.62)	1.7 (1.4, 2.1)	82 (66, 103)	27 (22, 33)
1200	5	0.42 (0.32, 0.56)	2.6 (2.3, 2.9)	112 (82, 153)	37 (27, 51)
3000	5	0.25 (0.21, 0.30)	4.2 (3.2, 5.5)	112 (79, 158)	37 (26, 52)
D-eflornithine					
40	5	1.1 (0.86, 1.5)	1.4 (1.2, 1.6)	195 (158, 241)	62 (50, 77)
150	5	1.1 (0.73, 1.6)	1.3 (1.1, 1.4)	184 (149, 228)	58 (47, 72)
400	6	1.1 (0.93, 1.3)	1.5 (1.1, 1.9)	189 (164, 218)	60 (52, 69)
1200	5	0.86 (0.67, 1.1)	2.6 (2.3, 2.9)	227 (168, 306)	72 (54, 97)
3000	5	0.46 (0.40, 0.54)	4.2 (3.2, 5.5)	200 (158, 252)	64 (50, 80)

*Data are presented as geometric mean values and 95% confidence intervals based on calculations from log-transformed parameters. Dose normalization of parameters was done in molar quantities for the dose each individual received. F, bioavailability was estimated by dose-normalised $AUC_{0-\infty}$ multiplied by the typical iv clearance value of 3.31 ml/min and 3.18 mL/min for L – and – D –eflornithine, respectively, for a typical rat weight of 338.4 grams.

Based on non-compartmental analysis, absorption of eflornithine enantiomers was linear in the dose range of 40 – 400 mg/kg bw (Table 6). At dose levels of 1200 and 3000 mg/kg bw a pronounced delay to reach maximum concentrations was observed. Based on deconvolution it was suggested that this was caused by a delay in time to reach maximum absorption rate and not by a saturated uptake across the gastrointestinal tract (Figure 10). This peak shift in time to reach maximum absorption rates, combined with that absorption rates did not reach a plateau, suggested that uptake of eflornithine enantiomers across the gastrointestinal tract, with this wider dose range, could not mechanistically be explained with the previous absorption model used in paper II. Possibly an active uptake was masked by other physiological processes, such as local gastrointestinal irritation.
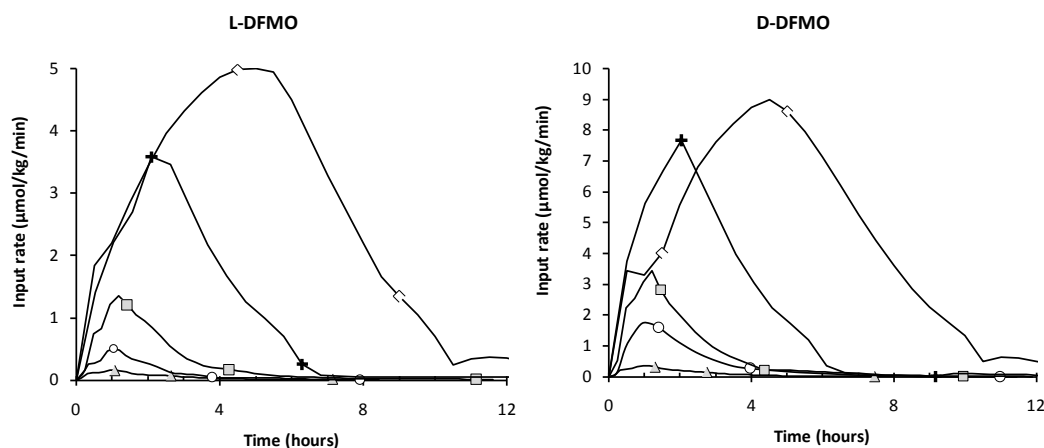

Figure 10. The geometric mean gastrointestinal input rate versus time after oral administration of 40 (Δ), 150 (O), 400 (□), 1200 (+) and 3000 (◊) mg/kg bodyweight of racemic eflornithine.

At donor enantiomeric concentrations of 0.75 and 12.5 mM, birectional permeability of eflornithine enantiomers across Caco-2 cells were low and did not show any clear signs of stereoselectivity (Table 7). The predicted human fraction absorbed from Caco-2 cell data was approximately 4%, using SimCYP ™ V.8.00 (Simcyp Limited©, Sheffield, UK). This underprediction suggested that there was an active absorption mechanism present *in vivo* not detectable in the present *in vitro* assay or that the paracellular route of absorption was the main route of gastrointestinal uptake of eflornithine enantiomers. However, the paracellular route was contradicted by the stereoselective process.

Table 7. Apparent permeability coefficients (P_{app}) for the transepithelial transport of L – and D – eflornithine across Caco-2 monolayers (24 – 25 days after Seeding) +

	Papp x 10^{-8} cm s^{-1} ± S.D.			
	L-DFMO		**D-DFMO**	
Donor enantiomeric concentration (mM)#	apical-to-basolateral	basolateral-to-apical	apical-to-basolateral	basolateral-to-apical
12.5	6.06 ± 1.31	10.61 ± 1.88	6.19 ± 1.32	10.61 ± 1.67
0.75	7.29 ± 0.16	8.93 ± 0.35	6.91 ± 0.22	8.11 ± 0.35
0.75 + GF120918*	7.35 ± 0.38	9.24 ± 0.38	6.99 ± 0.34	8.43 ± 0.39

+ measurements (n=3) done in HBSS at pH 7.4 on both the apical and basolateral side.

donor concentration is for each enantiomer when adding the racemic mixture.*the Pgp inhibitor GF120918 was present at concentrations of 10μM.

In summary this study showed that oral administration of racemic eflornithine in the rat resulted in a exposure to the *in vitro* more potent L – enantiomer being approximately 50% to that of the D – enantiomer. The bioavailability was more or less constant in the studied oral dose range. The differing bioavailabilities were not caused by presystemic metabolism, based on feces analysis, but rather stereoselective absorption across the gastrointestinal tract. Oral *in vivo* absorption data did not support an saturated active uptake the in gastrointestinal tract or that this mechanism was masked by other physiological processes. Data obtained from Caco-2 cells did not show any clear indications of stereoselectivity, efflux mechanisms or active uptake. Taken together, this study suggested that absorption of eflornithine may be subject to an active transporter not detectable or present in Caco-2 cell assays or that eflornithine is absorbed through the paracellular route. In the present analysis, the mechanism causing the stereoselective absorption could not be identified and further studies are required.

Stereoselective pharmacokinetics and pharmacodynamics of oral eflornithine against late-stage T.b.*gambiense* sleeping sickness – Paper V

Plasma pharmacokinetics after oral administration of racemic eflornithine was reasonably well described with a two-compartment disposition model with first order elimination. The absorption was described by a lag-time followed by first order absorption. Typical oral clearance (CL/F) values for L – and D – eflornithine were 17.6 (95%CI: 15.7, 19.5) and 8.18 (95%CI: 7.4, 8.96) L/h, respectively. Interindividual variability in clearance was reasonable low, 24% and 20% for L – and D – eflornithine, respectively. Absorption rate constants (ka) for L – and D – eflornithine were 0.448 and 0.437 h^{-1}, respectively. High between subject variability was observed in ka of 43.9 and 50%, for L – and D –

eflornithine, respectively. None of the covariates evaluated were shown to be significant (dose level, bodyweight, age, gender, concomitant medication, hemoglobin levels).

The difference in oral clearance for the enantiomers was clear, giving lower exposure of the L – enantiomer compared to the D – enantiomer. The difference in exposure was probably caused by a stereoselective absorption found in paper II and IV.
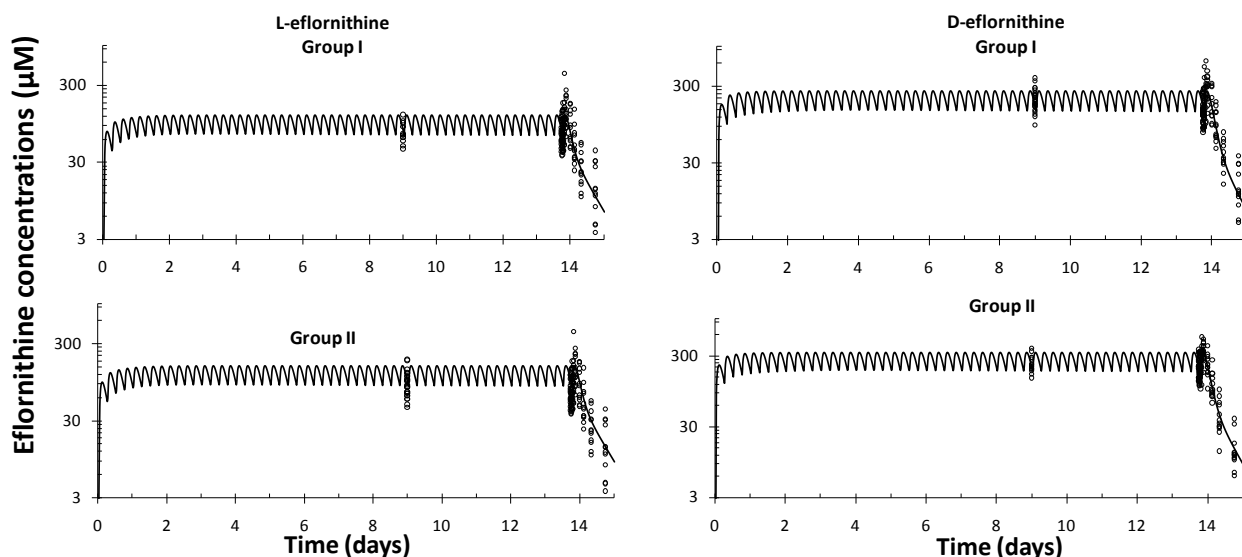

Figure 11. Experimental values for dose group I (100 mg/kg bw four times daily) and II (125 mg/kg bw four times daily) for L – (left panel) and D – eflornithine (right panel). The solid lines represent the population fit for L – and D – eflornithine, respectively.
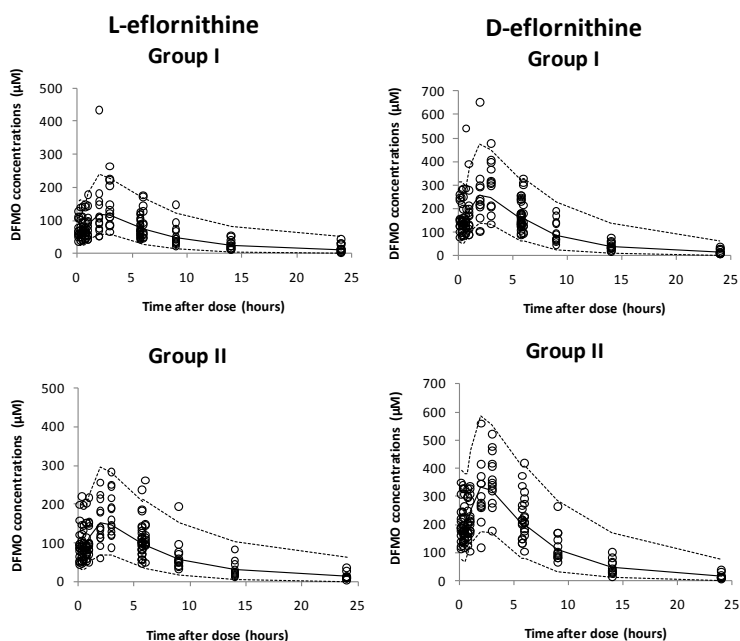

Figure 12. Visual predictive check of the final L – (left panel) and D – eflornithine (right panel) model according to treatment group. The circles are observed values. The dashed lines constitute a 95% prediction interval and the solid line is the median line predicted L – and D - eflornithine concentrations.

An unknown peak corresponding to the same retention time of the D – enantiomer was detected in blank CSF (*i.e.* prior to drug administration). This peak was on average 9% ± 8% (n=50, range: 1 – 36%, 95% CI: 7, 9%) of the measured level from day 10 and 15. The peak area eluting at the same retention time as the D – enantiomer was therefore subtracted from measured D – eflornithine concentrations on day 10 and 14. No peaks with the same retention time as for the L – enantiomer was detected. The mean concentration ratio between day 15 and day 10 were 0.99 (95% CI: 0.83, 1.15) and 0.99 (95% CI: 0.84, 1.16) for L – and D – eflornithine, respectively. Regressed CSF concentrations to plasma concentrations taken at the same time occasion, using origo as an intercept, gave slopes of 0.15 (95%CI: 0.13, 0.17) and 0.15 (95% CI: 0.13, 0.17) for L – and D – DFMO, respectively. Steady state CSF concentrations suggested that the transfer of eflornithine enantiomers into CSF was not a stereoselective process.

Of the 25 patients included in the study, six had recurring parasites within six months after ending treatment. In CSF, patients with concentrations below 23 µM and 68 µM for L – and total eflornithine, respectively, were more associated with having recurring parasites (Figure 13). For plasma $Css_{,min,}$ concentrations above 105 and 310 µM for L – and total eflornithine were cured. AUC_τ gave a significant correlation to the probability of being cured, although not more pronounced for the L – enantiomer compared to total eflornithine. Estimates based on bootstrapping 200 samples, corresponded to mean probability slopes of 0.00909 (95%CI: 0.00233, 0.0169) and 0.00424 (95 %CI: 0.0012, 0.00696) for L – and total eflornithine AUC_τ, respectively. Intercepts were -4.16 (95% CI: - 9.1, 0.606) and -7.17 (95%CI: -12.4, 0.467) for L – and total eflornithine, respectively.
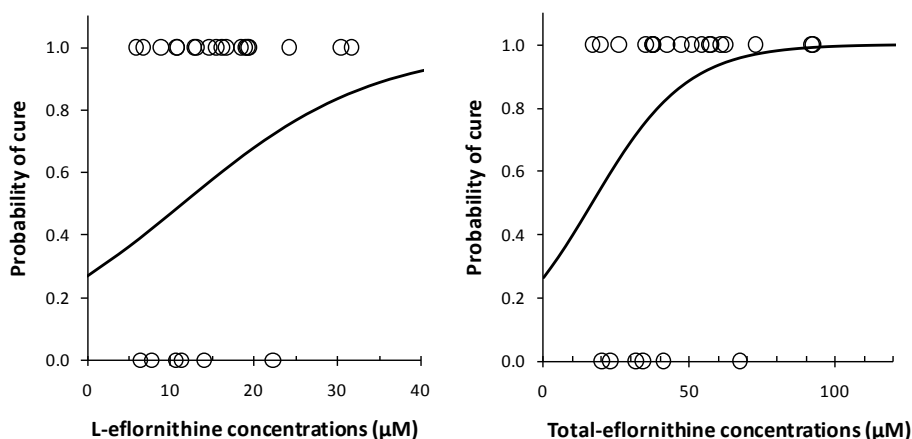

Figure 13. Logistic regression model. The probability of cure regressed against the average observed cerebrospinal fluid concentration, from day 10 and 14, for L – (left graph) and total eflornithine (right graph). D,L-eflornithine is the sum of L – and D – eflornithine concentrations. Circles are observed values and the solid line represents the predicted probability of being cured based on mean values from 200 bootstrap estimates. The probability of being cured against steady state CSF concentration were not statistically significant, based on 95% CI intervals of the probability slopes.
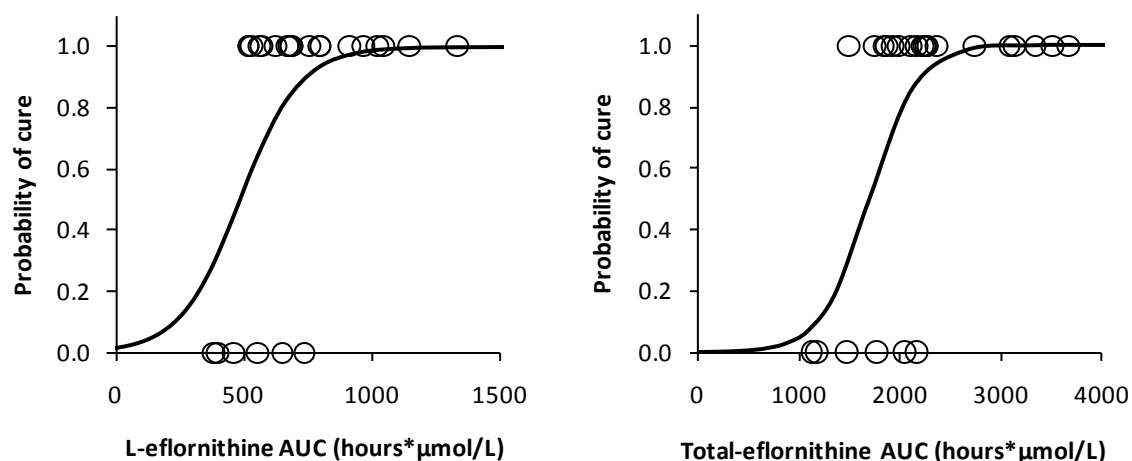
Figure 14. Logistic regression model. The probability of cure regressed against the predicted AUC in a dosing interval ($AUC_{0-6\ hours}$) for L − (left graph), and total eflornithine (right graph). Total eflornithine is the sum of L − and D − eflornithine concentrations. Circles are observed values and the solid line represents the predicted probability of being cured based on mean values from 200 bootstrap estimates. The correlation was significant (see text).

It has been suggested that total (D,L) eflornithine concentrations above 50 μM are required in CSF for a successful eradication of T.b.gambiense in humans [69, 80]. In the present study, steady state CSF concentration below 23 and 68 μM, for L- and D,L − eflornithine respectively, gave an inadequate response. AUC_τ gave a significant correlation to the probability of being cured, but not more pronounced for L − eflornithine compared to total eflornithine as exposure of the enantiomers were highly correlated.

To conclude, after oral administration of racemic eflornithine, different exposure to the separate enantiomers was apparent, probably caused by a stereoselective absorption across the gastrointestinal tract. The present findings may explain why an oral treatment of late-stage human African trypanosomiasis has failed and emphasizes that stereoselective pharmacokinetics needs to be considered when exploring the possibilities of developing an oral dosage regimen.

General discussion

The empirical method for prediction of Kp-values was developed with the intent to be used once an *in vivo* estimate of a volume of distribution has been obtained. The method was primarily developed for the implementation in whole body PBPK model simulations. However, in the case of eflornithine, a compound with a low transcellular permeability, a flow-limited distribution PBPK model could not simulate the terminal half life of eflornithine adequately. For a satisfactory PBPK model simulation of eflornithine, transcellular permeability rates would be needed, and each individual tissue would be needed to be divided into an extracellular and intracellular compartment. However, what became apparent during eflornithine experimental studies was that there were more relevant aspects that needed to be addressed. Therefore further studies were focused on the factors that were most critical for eflornithine from a clinical perspective.

Stereoselective absorption appears to be the challenging factor to address for the development of an oral eflornithine treatment against late-stage HAT. This is due to the low potency of eflornithine leading to the need of a high exposure, resulting in large doses. However, eflornithine is currently the most frequently recommended drug in lack of better treatment options. Although research is ongoing for finding alternative treatment options, eflornithine will most likely be the recommended treatment option for some years to come, either alone or in combination treatment.

The use of combination treatment for late-stage HAT should be further investigated. Nifurtimox combined with eflornithine appears to be a promising combination treatment in clinical trials[121, 122]. Preclinical studies have evaluated the possibility of increasing the low blood-brain permeability of eflornithine. Results show that suramin increase blood-brain barrier permeability of total eflornithine in the mouse [84]. Although, what ultimately would be needed is an oral treatment.

The possibilities of developing an oral treatment using eflornithine can probably not be solved by altering the dosage regimen. To enable an oral eflornithine treatment one would need to significantly increase the fraction absorbed. However, this would require further studies and in particular finding the mechanism that causes the stereoselective absorption. If the stereoselective absorption is driven is caused by an efflux mechanism the transporter might be inhibited by a selective inhibitor. If absorption is primarily driven by an active transporter lower doses (or only L-eflornithine) given more frequently might increase the bioavailability, and, if passive paracellular or transcellular absorption is the main mechanism, coadministration with permeability enhancers might be considered. In paper III, the absorption of eflornithine was investigated after oral administration to the rat covering a dose range of a factor 75. This wide dose range was applied to generate more information with regards to the stereoselective absorption. In addition Caco-2 cell studies were done to possibly find reasons for the disadvantageous stereoselective absorption. Based on the findings in this paper it was suggested that stereoselective absorption is either driven by an active transporter or that the paracellular route is the main route of absorption. Possibly, the gastrointestinal absorption of eflornithine is driven by several mechanisms, such as transcellular and or paracellular mechanisms and possibly

an active transport. However, for further studies of the gastrointestinal absorption of eflornithine more detailed studies are required.

Overall, this thesis has presented a novel method to predict tissue distribution and has investigated the stereoselective pharmacokinetics of eflornithine. The method to predict drug tissue distribution may aid the use of PBPK model simulations and may also be useful when comparing predicted tissue distributions to experimentally determined values. The results obtained for eflornithine provided knowledge that can contribute to a better understanding whether the development of an oral eflornithine treatment of late-stage HAT patients is feasible or not.

Conclusions

The present work can be concluded into:

- A method to predict drug specific tissue to plasma concentrations ratios has been developed, using a measured volume of distribution in combination with the compound lipophilicity.

- A sensitive and relatively simple method for determination of eflornithine enantiomers has been developed.

- After oral administration of racemic eflornithine to the rat the *in vitro* more potent L – enantiomer has an approximately 50 percent lower bioavailability compared to the D – enantiomer. The differing exposure is caused by stereoselective absorption in the gastrointestinal tract.

- The differing fraction absorbed has consequences for the development of an oral treatment of late stage human African trypanosomiasis infected patients. After oral administration to late stage-HAT patients the L – enantiomer has a higher oral clearance compared to the D – enantiomer, most likely caused by stereoselective absorption. Passage of eflornithine enantiomers into cerebrospinal fluid did not appear to be a stereoselective process. L – and total – eflornithine plasma exposure (AUC) gave, in the presented study of 25 patients, a significant correlation to the probability of being cured.

Acknowledgements

This work was performed at the Unit for Pharmacokinetics and Drug Metabolism, Department of Pharmacology, Institute of Neuroscience and Physiology, the Sahlgrenska Academy at University of Gothenburg. I am sincerely grateful to all the wonderful people that have made this thesis possible. I would especially express my gratitude and appreciation to the following persons:

My supervisor, Michael Ashton, for introducing me to the interesting field of pharmacokinetics, for your visionary ideas and most of all for giving me the opportunity to work within this field.

My co-supervisor, Sven Björkman, for constructive feedback and ideas, for sharing your knowledge and at the same time having a good sense of humor.

To the past and present members of the PKDM unit: Sara Asimus, Sofia Friberg Hietala, Sofia Sandberg, Carl Johansson, Dinko Rekic, Helena Dahlqvist and Emile Bienevue. A sincere gratitude for stimulating discussions and for the very nice social atmosphere. Special thanks to Carl for being very helpful and coping with me during our early morning and midnight lab work. Special thanks to Daniel Röshammar and your technical NONMEM advices, for the "creative" (=bizarre) discussions and for being a very supportive friend. Joel Tärning, for making me feel very welcome when I came to the PKDM unit, for your excellent entertaining capabilities and for your friendship. A big salute to Joel and Daniel for being the best comrades during congressing, in particular during the non-scientific activities.

Yngve Bergqvist, Susanne Römsing, Mikaela Malm and other members in the Borlänge analytical chemistry group. Thanks for all the stimulating discussion, for priceless help and advices during my research.

I am very grateful to Anna-Lena Ungell and Johan Gabrielsson for criticism and feedback provided during my half-time dissertation. Special thanks to Johan Gabrielsson for being very encouraging.

Mr C and Mrs N for helping me during periods of intensive workloads.

My sincere gratitude goes out to my project workers Carl Johansson, Christina Roth, Jenny Klint, and Veronika Sjöstrand for giving valuable input and help in my projects.

Special thanks goes out to Kenn Johannessen for lending me all the different tools when solving mechanical problems with the HPLC system.

This work was carried out in a friendly atmosphere with excellent friends, colleagues and hangarounds at "Pharmen". The friendship and all the social activities are greatly acknowledged. Special thanks goes out to Kim, Denny, Jocke, Mattias, Wolfan, and Röök.

My extended gratitude to my parents, Christina and Karl-Johan, for always believing in me and being there for me. My sister Lina, for making my life much more enjoyable and for your good sense of humor. My brother Patric, for your very supportive discussions and encouragement during though times. Gabriella and Jacobina for bringing much joy into my life.

To Gometz Gustafsson "imperiet": Christina, Reiner, Linn, Nina, Erik, Lars, Britt and Anna-Helga. Thank you for welcoming me into to your family and for your great support.

To all my fantastic friends, outside of the area of my research, for your help in keeping my life *almost* in balance: Victoria, Emma-Kajsa, Calle, Lisa, Erik, Carolina, Dave and Jonas.

Finally, this thesis would not have been possible without my *Cajsa*. Superlatives are not enough to describe how much I appreciate sharing my life with you. Nu är det vår tur.

References

1.   Gabrielsson J, Weiner D. Pharmacokinetic and Pharmacodynamic Data Analysis: Concepts and Applications, 4th ed. Swedish Pharmaceutical Society, Swedish Pharmaceutical Press, 2006.
2.   Kennedy PG. The fatal sleep. Luath Press Limited 2007.
3.   Simarro PP, Jannin J, Cattand P. Eliminating human African trypanosomiasis: where do we stand and what comes next? PLoS Med 5(2): e55, 2008.
4.   Burri C, Brun R. Eflornithine for the treatment of human African trypanosomiasis. Parasitol Res 90 Supp 1(S49-52, 2003.
5.   Qu N, Ignatenko NA, Yamauchi P, Stringer DE, Levenson C, Shannon P, Perrin S, Gerner EW. Inhibition of human ornithine decarboxylase activity by enantiomers of difluoromethylornithine. Biochem J 375(Pt 2): 465-70, 2003.
6.   Nestorov I. Whole body pharmacokinetic models. Clin Pharmacokinet 42(10): 883-908, 2003.
7.   Teorell T. Kinetics of distribution of substances administered to the body. Arch Int Pharmacodyn 57(205-240, 1937.
8.   Poulin P, Schoenlein K, Theil FP. Prediction of adipose tissue: plasma partition coefficients for structurally unrelated drugs. J Pharm Sci 90(4): 436-47, 2001.
9.   Poulin P, Theil FP. A priori prediction of tissue:plasma partition coefficients of drugs to facilitate the use of physiologically-based pharmacokinetic models in drug discovery. J Pharm Sci 89(1): 16-35, 2000.
10.   Poulin P, Theil FP. Prediction of pharmacokinetics prior to in vivo studies. II. Generic physiologically based pharmacokinetic models of drug disposition. J Pharm Sci 91(5): 1358-70, 2002.
11.   Poulin P, Theil FP. Prediction of pharmacokinetics prior to in vivo studies. 1. Mechanism-based prediction of volume of distribution. J Pharm Sci 91(1): 129-56, 2002.
12.   Berezhkovskiy LM. Volume of distribution at steady state for a linear pharmacokinetic system with peripheral elimination. J Pharm Sci 93(6): 1628-40, 2004.
13.   Rodgers T, Leahy D, Rowland M. Physiologically based pharmacokinetic modeling 1: predicting the tissue distribution of moderate-to-strong bases. J Pharm Sci 94(6): 1259-76, 2005.
14.   Rodgers T, Rowland M. Physiologically based pharmacokinetic modelling 2: predicting the tissue distribution of acids, very weak bases, neutrals and zwitterions. J Pharm Sci 95(6): 1238-57, 2006.
15.   Rodgers T, Rowland M. Mechanistic approaches to volume of distribution predictions: understanding the processes. Pharm Res 24(5): 918-33, 2007.
16.   Arundel P. A multi-compartment model generally applicable to physiologically based pharmacokinetics (AstraZeneca, UK) [poster]. In 3rd IFAC Symposium: modelling and control in biomedical systems,vol Warwick, UK, 1997.
17.   Jones HM, Parrott N, Jorga K, Lave T. A novel strategy for physiologically based predictions of human pharmacokinetics. Clin Pharmacokinet 45(5): 511-42, 2006.

18. Lapicque F, Muller N, Payan E, Dubois N, Netter P. Protein binding and stereoselectivity of nonsteroidal anti-inflammatory drugs. Clin Pharmacokinet 25(2): 115-23, 1993.

19. Mehvar R, Brocks DR, Vakily M. Impact of stereoselectivity on the pharmacokinetics and pharmacodynamics of antiarrhythmic drugs. Clin Pharmacokinet 41(8): 533-58, 2002.

20. Hamunen K, Maunuksela EL, Sarvela J, Bullingham RE, Olkkola KT. Stereoselective pharmacokinetics of ketorolac in children, adolescents and adults. Acta Anaesthesiol Scand 43(10): 1041-6, 1999.

21. Levy RH, Boddy AV. Stereoselectivity in pharmacokinetics: a general theory. Pharm Res 8(5): 551-6, 1991.

22. Kristensen K, Blemmer T, Angelo HR, Christrup LL, Drenck NE, Rasmussen SN, Sjogren P. Stereoselective pharmacokinetics of methadone in chronic pain patients. Ther Drug Monit 18(3): 221-7, 1996.

23. Augustijns P, Verbeke N. Stereoselective pharmacokinetic properties of chloroquine and de-ethyl-chloroquine in humans. Clin Pharmacokinet 24(3): 259-69, 1993.

24. Brocks DR, Mehvar R. Stereoselectivity in the pharmacodynamics and pharmacokinetics of the chiral antimalarial drugs. Clin Pharmacokinet 42(15): 1359-82, 2003.

25. Barissa GR, Poggi JC, Donadi EA, Dos Reis ML, Lanchote VL. Influence of rheumatoid arthritis in the enantioselective disposition of fenoprofen. Chirality 16(9): 602-8, 2004.

26. Wu CY, Benet LZ. Predicting drug disposition via application of BCS: transport/absorption/ elimination interplay and development of a biopharmaceutics drug disposition classification system. Pharm Res 22(1): 11-23, 2005.

27. He Y, Zeng, S. Determination of the stereoselectivity of chiral drug transport across Caco-2 cell monolayers. Chirality 18(1): 64-9, 2006.

28. Rowland M, Tozer TN. Clinical Pharmacokinetics: Concepts and Applications 3rd Edition. Lippincott Williams & Wilkins, 1989.

29. Stenberg P, Luthman K, Artursson P. Virtual screening of intestinal drug permeability. J Control Release 65(1-2): 231-43, 2000.

30. Lennernas H. Intestinal permeability and its relevance for absorption and elimination. Xenobiotica 37(10-11): 1015-51, 2007.

31. Cynober L. Pharmacokinetics of arginine and related amino acids. J Nutr 137(6 Suppl 2): 1646S-1649S, 2007.

32. Fagerholm U, Lindahl A, Lennernas H. Regional intestinal permeability in rats of compounds with different physicochemical properties and transport mechanisms. J Pharm Pharmacol 49(7): 687-90, 1997.

33. Lennernas H, Ahrenstedt O, Ungell AL. Intestinal drug absorption during induced net water absorption in man; a mechanistic study using antipyrine, atenolol and enalaprilat. Br J Clin Pharmacol 37(6): 589-96, 1994.

34. He YL, Murby S, Warhurst G, Gifford L, Walker D, Ayrton J, Eastmond R, Rowland M. Species differences in size discrimination in the paracellular pathway reflected by oral bioavailability of poly(ethylene glycol) and D-peptides. J Pharm Sci 87(5): 626-33, 1998.

35.	Fagerholm U, Borgstrom L, Ahrenstedt O, Lennernas H. The lack of effect of induced net fluid absorption on the in vivo permeability of terbutaline in the human jejunum. J Drug Target 3(3): 191-200, 1995.

36.	Lennernas H. Human intestinal permeability. J Pharm Sci 87(4): 403-10, 1998.

37.	Swaan PW. Recent advances in intestinal macromolecular drug delivery via receptor-mediated transport pathways. Pharm Res 15(6): 826-34, 1998.

38.	Berggren S, Gall C, Wollnitz N, Ekelund M, Karlbom U, Hoogstraate J, Schrenk D, Lennernas H. Gene and protein expression of P-glycoprotein, MRP1, MRP2, and CYP3A4 in the small and large human intestine. Mol Pharm 4(2): 252-7, 2007.

39.	Hilgendorf C, Ahlin G, Seithel A, Artursson P, Ungell AL, Karlsson J. Expression of thirty-six drug transporter genes in human intestine, liver, kidney, and organotypic cell lines. Drug Metab Dispos 35(8): 1333-40, 2007.

40.	Paine MF, Khalighi M, Fisher JM, Shen DD, Kunze KL, Marsh CL, Perkins JD, Thummel KE. Characterization of interintestinal and intraintestinal variations in human CYP3A-dependent metabolism. J Pharmacol Exp Ther 283(3): 1552-62, 1997.

41.	Madara JL. Regulation of the movement of solutes across tight junctions. Annu Rev Physiol 60(143-59, 1998.

42.	Chiba H, Osanai M, Murata M, Kojima T, Sawada N. Transmembrane proteins of tight junctions. Biochim Biophys Acta 1778(3): 588-600, 2008.

43.	Collett A, Walker D, Sims E, He YL, Speers P, Ayrton J, Rowland M, Warhurst G. Influence of morphometric factors on quantitation of paracellular permeability of intestinal epithelia in vitro. Pharm Res 14(6): 767-73, 1997.

44.	Proctor WR, Bourdet DL, Thakker DR. Mechanisms underlying saturable intestinal absorption of metformin. Drug Metab Dispos 36(8): 1650-8, 2008.

45.	Kerns EH. High throughput physicochemical profiling for drug discovery. J Pharm Sci 90(11): 1838-58, 2001.

46.	Epidemiology and control of African trypanosomiasis. Report of a WHO Expert Committee. World Health Organ Tech Rep Ser 739(1-127, 1986.

47.	Remme JH, Blas E, Chitsulo L, Desjeux PM, Engers HD, Kanyok TP, Kayondo JF, Kioy DW, Kumaraswami V, Lazdins JK, Nunn PP, Oduola A, Ridley RG, Toure YT, Zicker F, Morel CM. Strategic emphases for tropical diseases research: a TDR perspective. Trends Microbiol 10(10): 435-40, 2002.

48.	Kennedy PG. The continuing problem of human African trypanosomiasis (sleeping sickness). Ann Neurol 64(2): 116-26, 2008.

49.	Pepin J. Combination therapy for sleeping sickness: a wake-up call. J Infect Dis 195(3): 311-3, 2007.

50.	Control and surveillance of African trypanosomiasis. Report of a WHO Expert Committee. World Health Organ Tech Rep Ser 881(I-VI, 1-114, 1998.

51.	Human African trypanosomiasis (sleeping sickness): epidemiological update. Wkly Epidemiol Rec 81(8): 71-80, 2006.

52.	Kuzoe FA. Current situation of African trypanosomiasis. Acta Trop 54(3-4): 153-62, 1993.

53.	Kennedy PG. Human African trypanosomiasis-neurological aspects. J Neurol 253(4): 411-6, 2006.

54. Checchi F, Filipe JA, Barrett MP, Chandramohan D. The natural progression of gambiense sleeping sickness: what is the evidence? PLoS Negl Trop Dis 2(12): e303, 2008.

55. Docampo R, Moreno SN. Current chemotherapy of human African trypanosomiasis. Parasitol Res 90 Supp 1(S10-3, 2003.

56. Chappuis F. Melarsoprol-free drug combinations for second-stage Gambian sleeping sickness: the way to go. Clin Infect Dis 45(11): 1443-5, 2007.

57. Kibona SN, Matemba L, Kaboya JS, Lubega GW. Drug-resistance of Trypanosoma b. rhodesiense isolates from Tanzania. Trop Med Int Health 11(2): 144-55, 2006.

58. Brun R, Schumacher R, Schmid C, Kunz C, Burri C. The phenomenon of treatment failures in Human African Trypanosomiasis. Trop Med Int Health 6(11): 906-14, 2001.

59. Coyne PE, Jr. The eflornithine story. J Am Acad Dermatol 45(5): 784-6, 2001.

60. Ignatenko NA, Besselsen DG, Stringer DE, Blohm-Mangone KA, Cui H, Gerner EW. Combination chemoprevention of intestinal carcinogenesis in a murine model of familial adenomatous polyposis. Nutr Cancer 60 Suppl 1(30-5, 2008.

61. Gerner EW, Meyskens FL, Jr., Goldschmid S, Lance P, Pelot D. Rationale for, and design of, a clinical trial targeting polyamine metabolism for colon cancer chemoprevention. Amino Acids 33(2): 189-95, 2007.

62. Raul F. Revival of 2-(difluoromethyl)ornithine (DFMO), an inhibitor of polyamine biosynthesis, as a cancer chemopreventive agent. Biochem Soc Trans 35(Pt 2): 353-5, 2007.

63. Meyskens FL, Jr., McLaren CE, Pelot D, Fujikawa-Brooks S, Carpenter PM, Hawk E, Kelloff G, Lawson MJ, Kidao J, McCracken J, Albers CG, Ahnen DJ, Turgeon DK, Goldschmid S, Lance P, Hagedorn CH, Gillen DL, Gerner EW. Difluoromethylornithine plus sulindac for the prevention of sporadic colorectal adenomas: a randomized placebo-controlled, double-blind trial. Cancer Prev Res (Phila Pa) 1(1): 32-8, 2008.

64. Sporn MB, Hong WK. Clinical prevention of recurrence of colorectal adenomas by the combination of difluoromethylornithine and sulindac: an important milestone. Cancer Prev Res (Phila Pa) 1(1): 9-11, 2008.

65. Shapiro J, Lui H. Treatments for unwanted facial hair. Skin Therapy Lett 10(10): 1-4, 2005.

66. Bacchi CJ, Nathan HC, Hutner SH, McCann PP, Sjoerdsma A. Polyamine metabolism: a potential therapeutic target in trypanosomes. Science 210(4467): 332-4, 1980.

67. Balasegaram M, Harris S, Checchi F, Ghorashian S, Hamel C, Karunakara U. Melarsoprol versus eflornithine for treating late-stage Gambian trypanosomiasis in the Republic of the Congo. Bull World Health Organ 84(10): 783-91, 2006.

68. Balasegaram M, Young H, Chappuis F, Priotto G, Raguenaud ME, Checchi F. Effectiveness of melarsoprol and eflornithine as first-line regimens for gambiense sleeping sickness in nine Medecins Sans Frontieres programmes. Trans R Soc Trop Med Hyg 2008.

69. Milord F, Loko L, Ethier L, Mpia B, Pepin J. Eflornithine concentrations in serum and cerebrospinal fluid of 63 patients treated for Trypanosoma brucei gambiense sleeping sickness. Trans R Soc Trop Med Hyg 87(4): 473-7, 1993.

70. Checchi F, Piola P, Ayikoru H, Thomas F, Legros D, Priotto G. Nifurtimox plus Eflornithine for Late-Stage Sleeping Sickness in Uganda: A Case Series. PLoS Negl Trop Dis 1(2): e64, 2007.

71. Priotto G, Fogg C, Balasegaram M, Erphas O, Louga A, Checchi F, Ghabri S, Piola P. Three Drug Combinations for Late-Stage Trypanosoma brucei gambiense Sleeping Sickness: A Randomized Clinical Trial in Uganda. PLoS Clin Trials 1(8): e39, 2006.

72. Meyskens FL, Jr., Gerner EW. Development of difluoromethylornithine (DFMO) as a chemoprevention agent. Clin Cancer Res 5(5): 945-51, 1999.

73. Giffin BF, McCann PP, Bitonti AJ, Bacchi CJ. Polyamine depletion following exposure to DL-alpha-difluoromethylornithine both in vivo and in vitro initiates morphological alterations and mitochondrial activation in a monomorphic strain of Trypanosoma brucei brucei. J Protozool 33(2): 238-43, 1986.

74. Bitonti AJ, McCann PP, Sjoerdsma A. Necessity of antibody response in the treatment of African trypanosomiasis with alpha-difluoromethylornithine. Biochem Pharmacol 35(2): 331-4, 1986.

75. de Gee AL, McCann PP, Mansfield JM. Role of antibody in the elimination of trypanosomes after DL-alpha-difluoromethylornithine chemotherapy. J Parasitol 69(5): 818-22, 1983.

76. McCann PP, Bacchi CJ, Clarkson AB, Jr., Seed JR, Nathan HC, Amole BO, Hutner SH, Sjoerdsma A. Further studies on difluoromethylornithine in African trypanosomes. Med Biol 59(5-6): 434-40, 1981.

77. Doua F, Boa FY, Schechter PJ, Miezan TW, Diai D, Sanon SR, De Raadt P, Haegele KD, Sjoerdsma A, Konian K. Treatment of human late stage gambiense trypanosomiasis with alpha-difluoromethylornithine (eflornithine): efficacy and tolerance in 14 cases in Cote d'Ivoire. Am J Trop Med Hyg 37(3): 525-33, 1987.

78. Kazyumba GL, Ruppol JF, Tshefu AK, Nkanga N. [Arsenical resistance and difluoromethylornithine in the treatment of human African trypanosomiasis]. Bull Soc Pathol Exot Filiales 81(3 Pt 2): 591-4, 1988.

79. Taelman H, Marcelis L, Sonnet J, Kazyumba G, Van den Enden E, Wery M, Schechter PJ. [Treatment of human trypanosomiasis caused by Trypanosoma brucei gambiense using alpha-difluoromethylornithine. Results in 7 patients]. Bull Soc Pathol Exot Filiales 81(3 Pt 2): 578-88, 1988.

80. Milord F, Pepin J, Loko L, Ethier L, Mpia B. Efficacy and toxicity of eflornithine for treatment of Trypanosoma brucei gambiense sleeping sickness. Lancet 340(8820): 652-5, 1992.

81. Na-Bangchang K, Doua F, Konsil J, Hanpitakpong W, Kamanikom B, Kuzoe F. The pharmacokinetics of eflornithine (alpha-difluoromethylornithine) in patients with late-stage T.b. gambiense sleeping sickness. Eur J Clin Pharmacol 60(4): 269-78, 2004.

82. Levin VA, Byrd D, Campbell J, Davis RL, Borcich JK. CNS toxicity and CSF pharmacokinetics of intraventricular DFMO and MGBG in beagle dogs. Cancer Chemother Pharmacol 13(3): 200-5, 1984.

83. Levin VA, Csejtey J, Byrd DJ. Brain, CSF, and tumor pharmacokinetics of alpha-difluoromethylornithine in rats and dogs. Cancer Chemother Pharmacol 10(3): 196-9, 1983.

84. Sanderson L, Dogruel M, Rodgers J, Bradley B, Thomas SA. The blood-brain barrier significantly limits eflornithine entry into Trypanosoma brucei brucei infected mouse brain. J Neurochem 107(4): 1136-46, 2008.

85. Haegele KD, Alken RG, Grove J, Schechter PJ, Koch-Weser J. Kinetics of alpha-difluoromethylornithine: an irreversible inhibitor of ornithine decarboxylase. Clin Pharmacol Ther 30(2): 210-7, 1981.

86. Snyder Lloyd R. KJJ, Glajch Joseph L. Practical HPLC Method Development, second Edition. Wiley-Interscience Publication, 1997.

87. Malm M, Bergqvist Y. Determination of eflornithine enantiomers in plasma, by solid-phase extraction and liquid chromatography with evaporative light-scattering detection. J Chromatogr B Analyt Technol Biomed Life Sci 846(1-2): 98-104, 2007.

88. Ilisz I, Berkecz R, Peter A. Application of chiral derivatizing agents in the high-performance liquid chromatographic separation of amino acid enantiomers: a review. J Pharm Biomed Anal 47(1): 1-15, 2008.

89. Hanpitakpong W, Kamanikom B, Banmairuroi V, Na-Bangchang K. High-performance liquid chromatographic method for determination of 2-difluoromethyl-DL-ornithine in plasma and cerebrospinal fluid. J Chromatogr B Analyt Technol Biomed Life Sci 788(2): 221-31, 2003.

90. Hu T, Zuo H, Riley CM, Stobaugh JF, Lunte SM. Determination of alpha-difluoromethylornithine in blood by microdialysis sampling and capillary electrophoresis with UV detection. J Chromatogr A 716(1-2): 381-8, 1995.

91. Kilkenny ML, Slavik M, Riley CM, Stobaugh JF. Plasma analysis of alpha-difluoromethylornithine using pre-column derivatization with naphthalene-2,3-dicarboxaldehyde/CN and multidimensional chromatography. J Pharm Biomed Anal 17(6-7): 1205-13, 1998.

92. Smithers J. A precolumn derivatization high-performance liquid chromatographic (HPLC) procedure for the quantitation of difluoromethylornithine in plasma. Pharm Res 5(10): 684-6, 1988.

93. Cohen JL, Ko RJ, Lo AT, Shields MD, Gilman TM. High-pressure liquid chromatographic analysis of eflornithine in serum. J Pharm Sci 78(2): 114-6, 1989.

94. Wagner J, Gaget C, Heintzelmann B, Wolf E. Resolution of the enantiomers of various alpha-substituted ornithine and lysine analogs by high-performance liquid chromatography with chiral eluant and by gas chromatography on Chirasil-Val. Anal Biochem 164(1): 102-16, 1987.

95. US-FDA. Bioanalytical Method Validation Guidance. Food and Drug Administration, Center for Drug Evaluation and Research, 2001

96. WinNonlin version 5.2. In Mountain View, California, USA, Pharsight,

97. Kwon Y. Handbook of Essential Pharmacokinetics, Pharmacodynamics, and Drug Metabolism for Industrial Scientists. New York, Kluwer Academic/Plenum Publischers, 2001.

98. Ette EI, Williams PJ, Kim YH, Lane JR, Liu MJ, Capparelli EV. Model appropriateness and population pharmacokinetic modeling. J Clin Pharmacol 43(6): 610-23, 2003.

99. Box GEP. Robustness in the strategy of scientific model building strategy, Robustness in Statistics. In Laurel RL and Wilkinson GE.,vol Academic Press, New York, 1979: p.201-36, 1979.

100. Sheiner LB. The population approach to pharmacokinetic data analysis: rationale and standard data analysis methods. Drug Metab Rev 15(1-2): 153-71, 1984.

101. Dartois C, Brendel K, Comets E, Laffont CM, Laveille C, Tranchand B, Mentre F, Lemenuel-Diot A, Girard P. Overview of model-building strategies in population PK/PD analyses: 2002-2004 literature survey. Br J Clin Pharmacol 64(5): 603-12, 2007.

102. Karlsson MO, Holford, N. . A tutorial on visual predictive checks. In PAGE Meeting,vol Marseille, France, 2008.

103. Bouzom F, Laveille C, Merdjan H, Jochemsen R. Use of nonlinear mixed effect modeling for the meta-analysis of preclinical pharmacokinetic data: application to S 20342 in the rat. J Pharm Sci 89(5): 603-13, 2000.

104. Tunblad K, Hammarlund-Udenaes M, Jonsson EN. Influence of probenecid on the delivery of morphine-6-glucuronide to the brain. Eur J Pharm Sci 24(1): 49-57, 2005.

105. Jonsson EN, Wade JR, Karlsson MO. Nonlinearity detection: advantages of nonlinear mixed-effects modeling. AAPS PharmSci 2(3): E32, 2000.

106. Bjorkman S. Prediction of the volume of distribution of a drug: which tissue-plasma partition coefficients are needed? J Pharm Pharmacol 54(9): 1237-45, 2002.

107. SPSS Statistics 16.0. In Chicago, Illinois, USA, SPSS Inc., 2006.

108. Norman R. Draper HS. Applied regression analysis. New York, JOHN WILEY & SONS, INC., 1998.

109. Beal SL SL, Boeckmann AJ. NONMEM Users Guides 1989-2006, Icon Developments Solutions, Elliot City, MD, USA. In

110. Census, version 1.0. In Bazel, Switzerland, Novartis, Pharma AG,

111. Lindbom L, Pihlgren P, Jonsson EN. PsN-Toolkit--a collection of computer intensive statistical methods for non-linear mixed effect modeling using NONMEM. Comput Methods Programs Biomed 79(3): 241-57, 2005.

112. Leo A. Partition Coefficients and Their uses. Chemical Reviews 71(6): 525 - 616, 1971.

113. Sawada Y, Hanano M, Sugiyama Y, Harashima H, Iga T. Prediction of the volumes of distribution of basic drugs in humans based on data from animals. J Pharmacokinet Biopharm 12(6): 587-96, 1984.

114. Bernareggi A, Rowland M. Physiologic modeling of cyclosporin kinetics in rat and man. J Pharmacokinet Biopharm 19(1): 21-50, 1991.

115. Savic RM, Jonker DM, Kerbusch T, Karlsson MO. Implementation of a transit compartment model for describing drug absorption in pharmacokinetic studies. J Pharmacokinet Pharmacodyn 34(5): 711-26, 2007.

116. Wilkins JJ, Savic RM, Karlsson MO, Langdon G, McIlleron H, Pillai G, Smith PJ, Simonsson US. Population pharmacokinetics of rifampin in pulmonary tuberculosis patients, including a semimechanistic model to describe variable absorption. Antimicrob Agents Chemother 52(6): 2138-48, 2008.

117. Osterberg O, Savic RM, Karlsson MO, Simonsson US, Norgaard JP, Walle JV, Agerso H. Pharmacokinetics of desmopressin administrated as an oral lyophilisate dosage form in children with primary nocturnal enuresis and healthy adults. J Clin Pharmacol 46(10): 1204-11, 2006.

118. US-FDA. Bioanalytical Method Validation Guidance. In Food and Drug Administration, Center for Drug Evaluation and Research, 2001.

119. Gueorguieva I, Nestorov IA, Murby S, Gisbert S, Collins B, Dickens K, Duffy J, Hussain Z, Rowland M. Development of a whole body physiologically based model to characterise the pharmacokinetics of benzodiazepines. 1: Estimation of rat tissue-plasma partition ratios. J Pharmacokinet Pharmacodyn 31(4): 269-98, 2004.

120. Funk C. The role of hepatic transporters in drug elimination. Expert Opin Drug Metab Toxicol 4(4): 363-79, 2008.

121. Priotto G, Kasparian S, Mutombo W, Ngouama D, Ghorashian S, Arnold U, Ghabri S, Baudin E, Buard V, Kazadi-Kyanza S, Ilunga M, Mutangala W, Pohlig G, Schmid C, Karunakara U, Torreele E, Kande V. Nifurtimox-eflornithine combination therapy for second-stage African Trypanosoma brucei gambiense trypanosomiasis: a multicentre, randomised, phase III, non-inferiority trial. Lancet 374(9683): 56-64, 2009.

122. Opigo J, Woodrow C. NECT trial: more than a small victory over sleeping sickness. Lancet 374(9683): 7-9, 2009.